Journal of Palaeogeography

ORIGINAL ARTICLE Open Access

Diversified calcimicrobes in dendrolites of the Zhangxia Formation, Miaolingian Series (Middle Cambrian) of the North China craton

Ming-Xiang Mei[1,2], Muhammad Riaz[3,4,5*], Zhen-Wu Zhang[1], Qing-Fen Meng[1] and Yuan Hu[1]

Abstract

As a type of non-laminated microbial carbonates, dendrolites are dominated by isolated dendritic clusters of calcimicrobes and are distinct from stromatolites and thrombolites. The dendrolites in the upper part of the Miaolingian Zhangxia Formation at Anjiazhuang section in Feicheng city of Shandong Province, China, provide an excellent example for further understanding of both growth pattern and forming mechanism of dendrolites. These dendrolites are featured by sedimentary fabrics and composition of calcified microbes as follows. (1) The strata of massive limestones, composed of dendrolites with thickness of more than one hundred meters, intergrade with thick-bedded to massive leiolites, formimg the upper part of a third-order depositional sequence that constitutes a forced regressive systems tract. (2) A centimeter-sized bush-like fabric (shrub) typically produced by calcified microbes is similar to the mesoclot in thrombolites but distinctive from clotted fabrics of thrombolites. This bush-like fabric is actually constituted by diversified calcified microbes like the modern shrub as a result of gliding mobility of filamentous cyanobacteria. Such forms traditionally include: the *Epiphyton* group (which actually has uncertain biological affinity), the *Hedstroemia* group which closely resembles modern rivulariacean cyanobacteria, and the possible calcified cyanobacteria of the *Lithocodium–Bacinella* group. (3) Significantly, dense micrite of leiolite is associated with sponge fossils and burrows, and is covered by microstromatolite. The *Lithocodium–Bacinella* group is a controversial group of interpreted calcified cyanobacteria in the Cambrian that has also been widely observed and described in the Mesozoic. Therefore, dendrolites with symbiosis of leiolites in the studied section provide an extraordinary example for further understanding of growing style of bush-like fabrics (shrubs) of the dendrolites dominated by cyanobacterial mats. Furthermore, the present research provides some useful thinking approaches for better understanding of the history of the Early Paleozoic skeletal reefs and the microbe–metazoan transitions of the Cambrian.

Keywords: Calcified microbe, Dendrolite, Leiolite, *Epiphyton*, *Lithocodium–Bacinella*, Cambrian, Miaolingian, Zhangxia Formation

* Correspondence: riazjass@yahoo.com
[3]State Key Laboratory of Oil and Gas Reservoir Geology and Exploitation, Chengdu University of Technology, Chengdu 610059, China
[4]College of Energy Resources, Chengdu University of Technology, Chengdu 610059, China
Full list of author information is available at the end of the article

1 Introduction

Although microbialites (Burne and Moore 1987) are formed by the action or influence of microbes, they do not always preserve direct, or diagenetically robust, evidence for their mode of formation, thus, they are believed to be among the most intractable sedimentary rocks to study (Bosence et al. 2015). Microbial carbonates (calcified microbialites) are the spectacular examples of "microbially-induced sedimentary structures" (MISSs; Noffke and Awramik 2013). Microbial carbonates have been classified into four types on the basis of mesostructure, i.e. stromatolites marked by laminated structures, thrombolites associated with clotted fabrics, leiolites commonly expressed as structureless, and dendrolites characterized by dendritic fabrics (Burne and Moore 1987; Riding 1991a, 2000, 2011a).

Among a variety of microbial sedimentary structures in carbonates, dendrolite is characterized by the following particularities and complexities (Riding 1991a). Firstly, the dendrolites have a non-laminated mesostructure with relatively large (cm scale) clots dominated by isolated dendritic clusters of calcimicrobes (mainly grouped into *Epiphyton*; Riding 1991a, 2000; Howell et al. 2011). Dendrolites are commonly confused with thrombolites due to similar clotted fabrics (Chen et al. 2014a, 2014b; Gong 2016; Yan et al. 2017), and defined as dendritic thrombolite (Qi et al. 2014), *Epiphyton* framstone (Han et al. 2009), or *Epiphyton* buildup (Woo et al. 2008; Woo and Chough 2010). Secondly, similar to the modern dendrolitic cone (Bradley et al. 2017) or dendrolitic microbial mat (Suosaari et al. 2018), the dendrolites of the Cambrian are dominated by diversified filamentous microbes. Thirdly, it seems that dendrolites have a distinctive distribution during the Cambrian Miaolingian (Riding 2000; Rowland and Shapiro 2002). The reason for the special temporal distribution is not still throughly understood. Fourthly, the biological affinity of the main calcimicrobes belonging to the *Epiphyton* group in the Cambrian dendrolites remains uncertain (Riding 1991b, 1991c, 2011b; Luchinina and Terleev 2008, 2014; Luchinina 2009).

The common calcimicrobes belong to the *Epiphyton* group, the *Hedstroemia* group, and the *Lithocodium*–*Bacinella* group. Although results of several reseachers demonstrated that biological affinity of fossils of the *Epiphyton* group belongs to the cyanobacteria (e.g. Zhang et al. 1985; Jiang and Sha 1996; Laval et al. 2000; Woo et al. 2008; Han et al. 2009; Woo and Chough 2010; Chen et al. 2014a, 2014b; Săsăran et al. 2014; Gong 2016; Ezaki et al. 2017), some researchers did not include it in cyanobacteria (Luchinina and Terleev 2008, 2014; Luchinina 2009; Adachi et al. 2014, 2015; Liu et al. 2016). There are numerous arguments about the affilation of calcified cyanobacteria with the *Lithocodium*–*Bacinella* group (Cherchi and Schroeder 2006; Rameil et al. 2010; Schlagintweit and Bover-Arnal 2013). The sedimentary fabrics of the studied Cambrian microbial reefs show similar characteristics to the *Lithocodium* that either formed through decomposition of sponges (Kwon et al. 2012; Chen et al. 2014a, 2014b; Lee et al. 2014a, 2014b, 2015; Li et al. 2015; Park et al. 2015; Coulson and Brand 2016; Shen and Neuweiler 2018; Cordie et al. 2019) or from sponge fibers of keratose demosponges (Luo and Reitner 2014, 2016; Coulson and Brand 2016; Lee and Riding 2018; Shen and Neuweiler 2018; Lee et al. 2019). These arguments enhance the sophistication of the studied Middle Cambrian dendrolites at the Anjiazhuang section that provides an example for further understanding of the growth pattern and forming mechanism of calcified microbes. Furthermore, the establishment of the *Lithocodium* or *Lithocodium*-like fabric in the Cambrian dendrolites on the North China craton may provide some useful thinking approaches and research clues for further research of the early history of the Paleozoic skeletal reefs (Rowland and Shapiro 2002; Kiessling 2009; Lee et al. 2015, 2019; Ezaki et al. 2017; Lee and Riding 2018; Cordie et al. 2019) and the microbe–metazoan transitions (Chen et al. 2019).

2 Geological setting

Phanerozoic sedimentation in the North Chia craton began in Cambrian Epoch 2 times. The Cambrian sediments unconformably overlie the Precambrian sediments in a similar style as described in North America (Peters and Gaines 2012). Consequently, approximately 700 m thick Cambrian strata were deposited on the North China Platfrom, consisting of a mixed sucession of red beds and carbonate rocks from late part of Epoch 2 to early Miaolingian, a carbonate succession dominated by oolitic grainstones during the main period of the Miaolingian, and a succession of carbonate rocks predominated by carbonate mud during the Furongian (Wang et al. 1989; Meng et al. 1997; Shi et al. 1997; Feng et al. 2004; Mei 2011a; Ma et al. 2017; Latif et al. 2018; Riaz et al. 2019a, 2019b).

The Miaolingian Series in the North China craton comprises Maozhuang, Xuzhuang, Zhangxia and Gushan formations (e.g. Peng and Zhao 2018), and can be subdivided into four third-order depositional sequences (Ma et al. 2017; Latif et al. 2018; Riaz et al. 2019a, 2019b). The oolitic-grain bank that developed during the forced regression (Fig. 1) laid the foundation of ramp-type carbonate platform (see Pratt et al. 2012). It is characterized by shallow shelf ooidal shoals, flanked seawards by a ramp and landwards by tidal flats (Fig. 2a) (e.g. Feng et al. 1990, 2004; Meng et al. 1997). Moreover, abundant microbial reefs (Riding 2002a; Rowland and Shapiro 2002; Kiessling 2009; Chen et al. 2014a, 2014b; Lee et al.

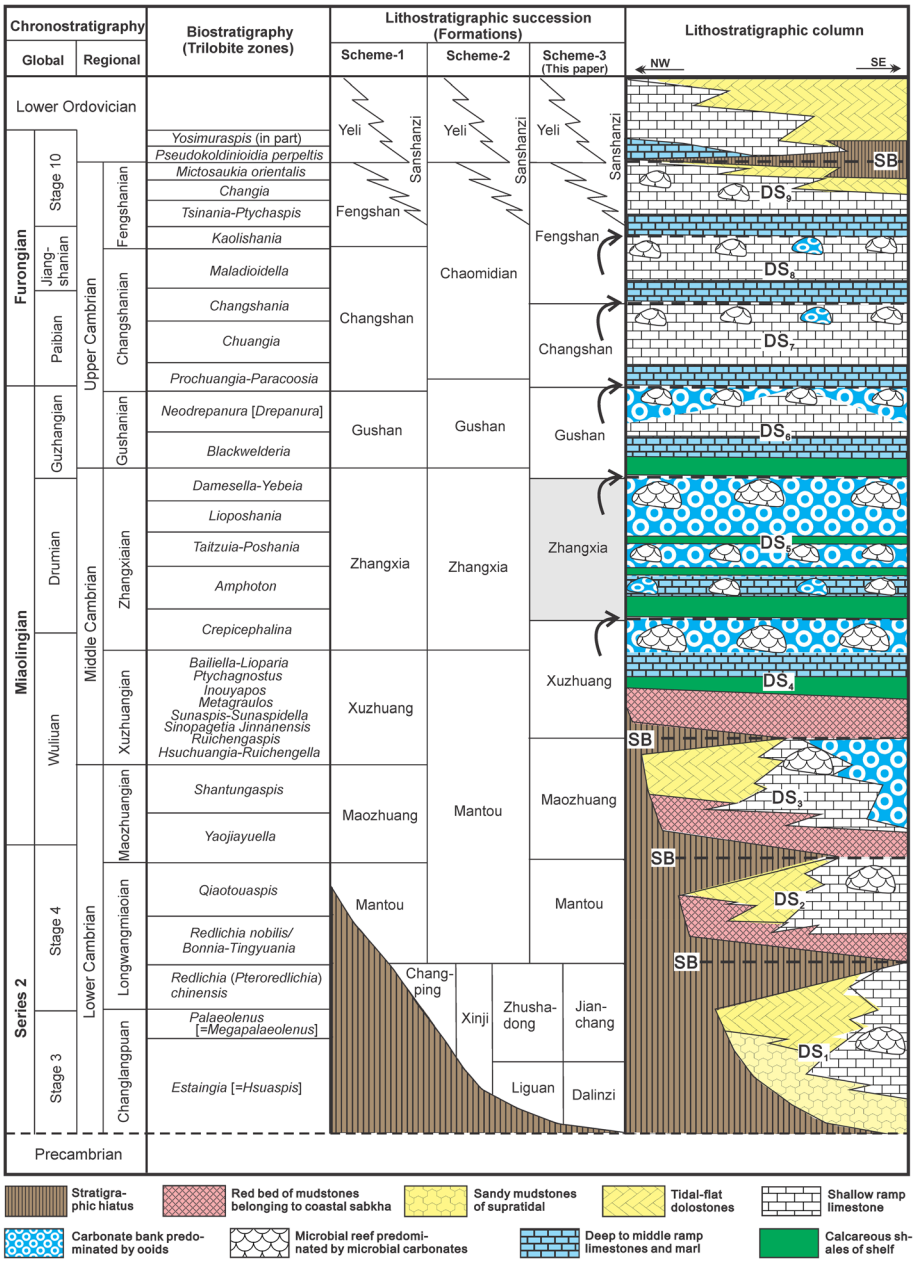

Fig. 1 Diagram depicts the sedimentary succession of the Cambrian in North China craton. Biostratigraphic succession of trilobites is adapted from Peng (2009). The scheme-1 for the lithostragraphic division is adapted from Lu et al. (1994), Meng et al. (1997) and Feng et al. (1990, 2004). Scheme-2 is from Xiang et al. (1999). Scheme-3 is used in present paper, and is modified from scheme-1 on the basis of sequence-stratigraphic division according to succession of sedimentary facies. Nine third-order sequences (DS_1 to DS_9) are discerned in the Cambrian System in the North China craton, which are divided by two types of sequence boundaries, i.e. the exposure punctuated surface (SB) and the drowning unconformity surface (arrows). The gray rectangle marks the target strata in present study

2014a, 2014b, 2015, 2019; Lee and Riding 2018; Cordie et al. 2019) dominated by microbial carbonates were developed in the shallow shelf covered by ooidal shoals (Fig. 2a), which are similar to "algal flats" (Jiang and Sha 1996; Sha and Jiang 1998).

Similar to other regions of the North China craton, the Zhangxia Formation at the Anjiazhuang section in the western part of Shandong Province consists of a third-order sequence (DS_5: Fig. 1) that is further subdivided into three subsequences (I to III in Fig. 3). The top and bottom of each subsequence is marked by drowning unconformities (e.g. Schlager 1989, 1999; Gómez and Fernández-López 1994; Mei 1996, 2010). These boundaries depict rapid transgressions by directly overlying

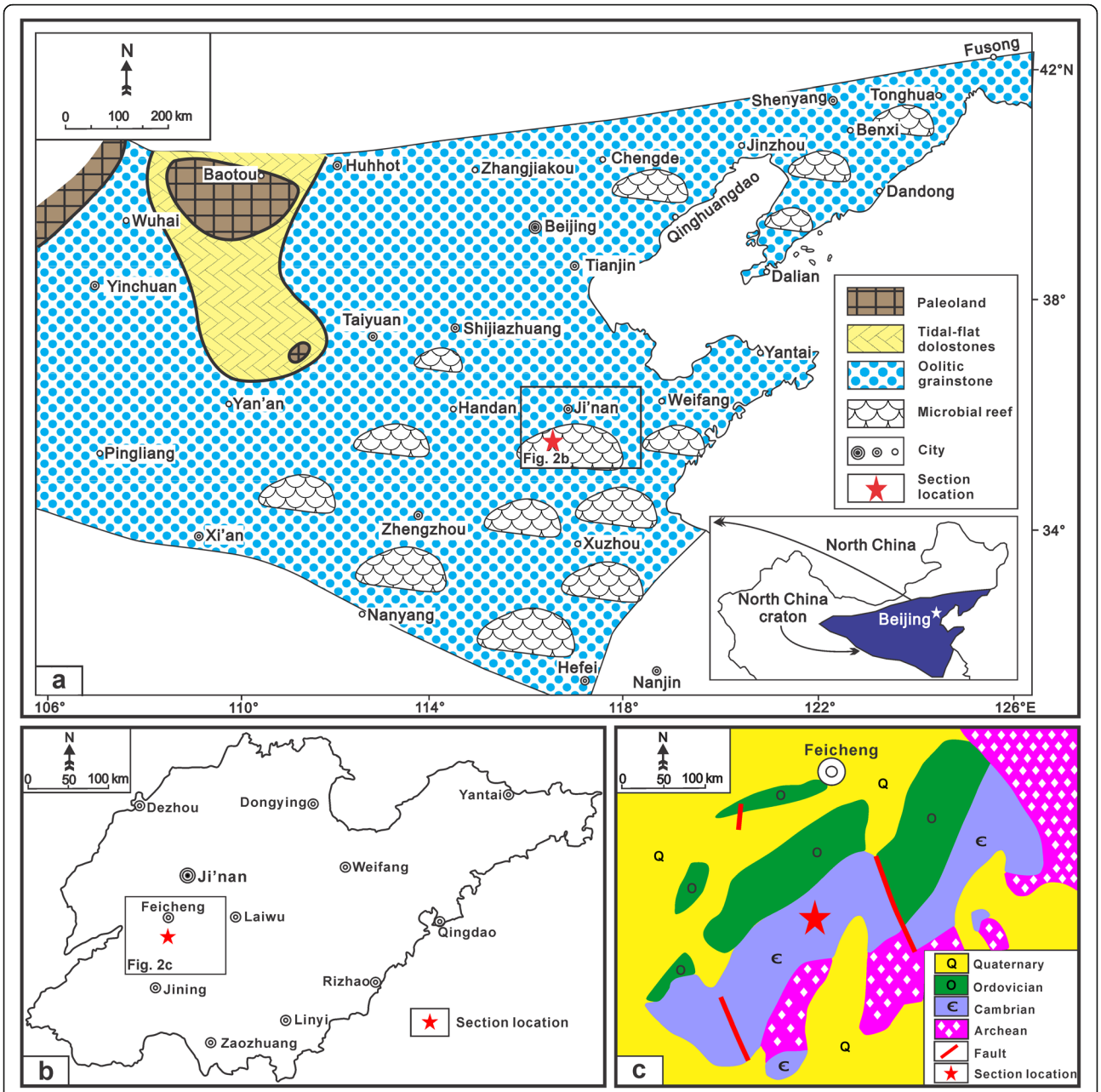

Fig. 2 **a** Sedimentary pattern for the late depositional period of the Cambrian Miaolingian Zhangxia Formation in the North China craton (adapted from Feng et al. 1990, 2004); **b** Geographical outline of Shandong Province with the section location; **c** Regionally geological feature in the southern part of Feicheng city with the section location

shelf mudstones on high-energy oolitic grainstones with the intergrowth of massive bioherms comprising microbial carbonates. The strata in the upper part of subsequence III of the Zhangxia Formation at the studied section, recording the relative sea-level fall, can be distinguished into three parts (b, c, and e in Fig. 3a): (1) the lower part is marked by a set of oncolitic- and oolitic-grainstones with thickness of about 15 m (Fig. 3b); (2) the middle part is constituted by a set of massive oolitic grainstones with approximately thickness is 30 m (Fig. 3c); (3) the upper part is about 125 m thick and comprises of massive biohermal limestones dominated by dendrolites with the intergrowth of leiolites (Fig. 3e), which is the key target of this study. These are remarkable deposits especially for the diversified cyanobacteria composition and the heterogeneous sedimentary fabrics in dendrolites with the intergrowth of leiolites, which further fit the concept of microbial reefs (Rowland and Shapiro 2002; Kiessling 2009; Lee et al. 2014a, 2014b, 2015, 2019; Lee and Riding 2018; Cordie et al. 2019).

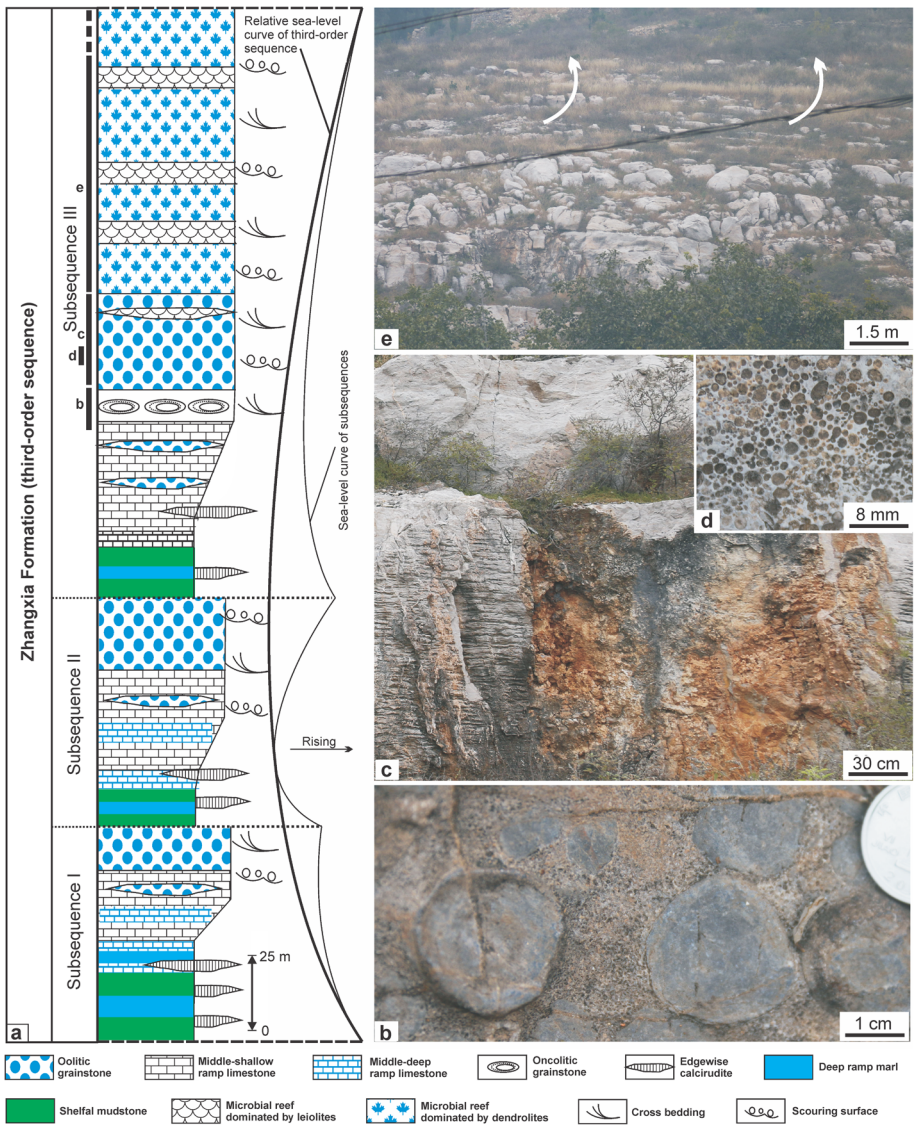

Fig. 3 Shoaling-upward succession of the Miaolingian Zhangxia Formation at the Anjiazhuang section (location is shown in Fig. 2). **a** The succession consists of a third-order sequence (equals to DS_5 in Fig. 1) which is further subdivided into three subsequences (I to III, as seprated by dotted lines). The upper part of subsequence III comprises three parts, i.e., **b**, **c**, and **e**, upwards, representing three types of carbonate rocks as follows; **b** Oncolitic- and oolitic-grainstones; **c**, **d** Massive oolitic grainstones; **e** Massive limestones dominated by dendrolites with the intergrowth of leiolites, which is the key target of this study

3 Materials and methods

Dendrolites with the intergrowth of leiolites in the massive limestones are most abundant in the upper part of subsequence III of the Miaolingian Zhangxia Formation at the Anjiazhuang section (Figs. 2, 3). The macro- and mesostructures of these massive limestones were observed on pale weathered surfaces (Fig. 3e). Detailed observations were conducted on the well-exposed outcrops, where 118 samples were collected from massive limstones, oolitic grainstone and oncolitic grainstone. Microfabrics were observed in thin sections with a Zeiss Axio Scope A1 microscope. High-resolution images were made for dendrolites and leiolites under the microscope.

4 Results

4.1 Fundamental features of the dendrolite

4.1.1 Macroscopic feature

The term dendrolite was firstly introduced by Riding (1991a). It has a distinctive form different from the laminated stromatolite and clotted thrombolite (Riding 1991a, 2000). Typical samples of dendrolites were collected from the Miaolingian Zhangxia Formation at the Anjiazhuang section in the western part of Shandong Province (Fig. 2b).

Macroscopically, the dendrolites of the Zhangxia Formation at the Anjiazhuang section are composed of large-scale (cm-sized) and small-scale (mm-sized) dark

clots of dense micrites (Fig. 4). These clots verify the initial definition of thrombolite (Aitken 1967) that led to an important distinction between thrombolites and stromatolites (Kennard and James 1986). These special clots are bush-like (shrubs), and are made up of isolated dendritic clusters of calcimicrobes (including *Epiphton*), which occur in the following forms: (1) irregular bodies of semi-connected or isolated shape (Fig. 4a), (2) relatively regular bodies of large-scale fan-like or chamber-like shape (cm-sized; Fig. 4b), and (3) small-scale (mm-sized) regular or irregular isolated bodies of chamber-like shape (Fig. 4c).

4.1.2 Microscopic feature

Diversified calcimicrobe composition and heterogeneous sedimentary fabrics in dendrolites of the Miaolingian Zhangxia Formation are shown in Figs. 5, 6, 7, 8, 9, 10. The bush-like fabrics (or shrubs) of the dendrolites in mm- to cm-level size are made up of isolated dendritic clusters of calcimicrobes (Figs. 5, 6, 7, 8, 9, 10). Microscopically, these calcimicrobes belong to fossils of the *Epiphyton* group (Riding 1991b, 1991c, 2000; Luchinina and Terleev 2008, 2014; Woo et al. 2008; Han et al. 2009; Luchinina 2009; Woo and Chough 2010; Yan et al. 2017) with lengths up to 500 μm and diameters from 50 μm to 70 μm, and depict the structure of bifurcating branches of dense micritic rods. These typical fossils of the *Epiphyton* commonly form cm-size or even larger shrub thalli (Fig. 5a), fan-like thalli (Fig. 5b), and isolated chamber-like thalli (Fig. 5c). The *Epiphyton* along with *Korilophyton* ("K" in Fig. 5c, d; solid micrite, but with short branches; Riding 1991b, 1991c) can form isolated chamber-like thalli. These thalli of calcimicrobes seem to grow in a matrix of dense micrites as well as a particular matrix of microspars that are similar to the "*Bacinella*-like" fabric (Schlagintweit and Bover-Arnal 2013) or the *Bacinella* (Cherchi and Schroeder 2006; Rameil et al. 2010).

More importantly, four special microfabrics are observed within the dendrolites (Fig. 5). Firstly, it is the possible *Lithocodium* (Cherchi and Schroeder 2006; Rameil et al. 2010; Schlagintweit and Bover-Arnal 2013) which shows the characteristic of microtubular fabric in dark dense micrites. The dark micritic aggregations are

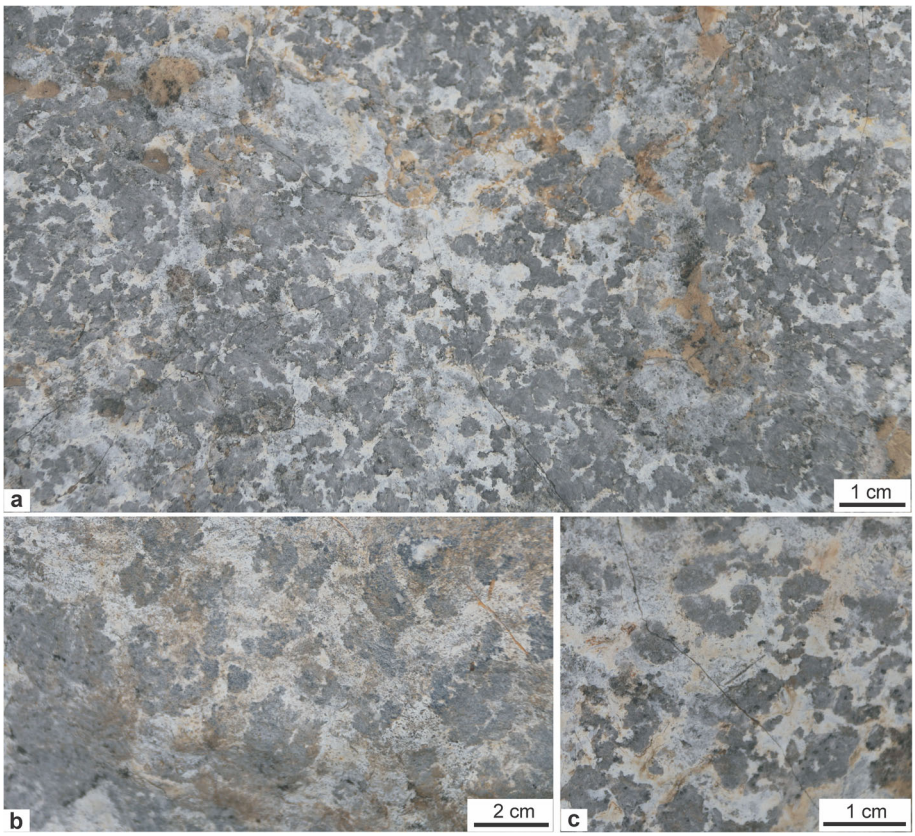

Fig. 4 Macroscopic photographs of the dendrolites in top part of the subsequence III of the Zhangxia Formation at the Anjiazhuang section, Shandong Province. These isolated dendritic clusters of calcimicrobes are composed of dense dark micrites similar to mesoclots defined by Aitken (1967), and can generally be subdivided into three types: **a** Irregular bodies of semi-connected or isolated shape; **b** Relatively regular bodies of large-scale fan-like or chamber-like shape; and **c** Small-scale (mm-sized) regular or irregular isolated bodies of chamber-like shape

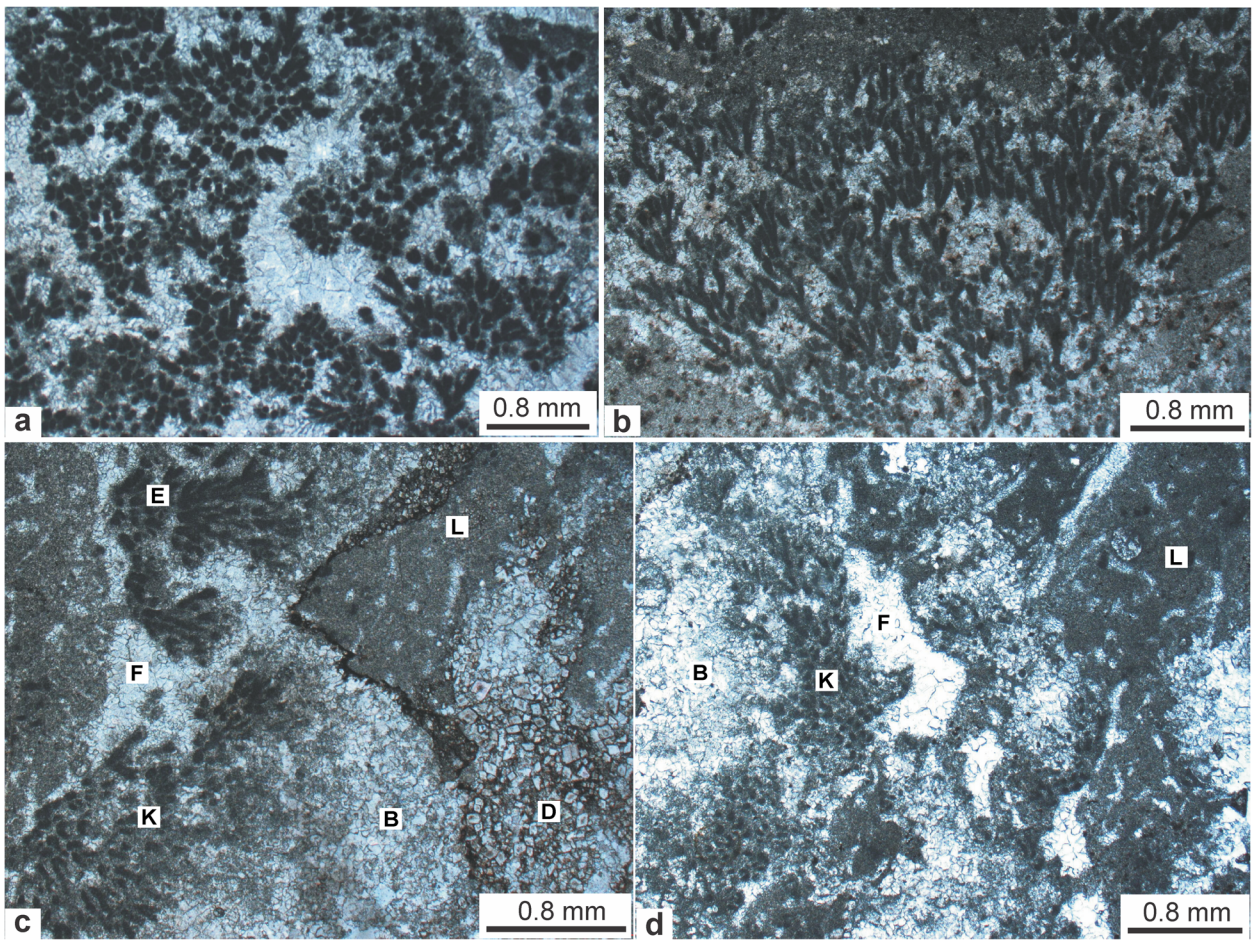

Fig. 5 Photomicrographs of the dendrolites in the top part of the subsequence III of the Zhangxia Formation at the Anjiazhuang section, Shandong Province. The fabrics vary along with the types of calcified cyanobacteria. **a** The large-scale shrub-like thalli composed of typical *Epiphyton*; **b** Fan-like thalli composed of typical *Epiphyton*; **c** Chamber-shaped thalli composed of typical *Epiphyton* (E) and *Korilophyton* (K) with possible *Lithocodium* (L), dolomitic cement (D), and fenestral cavities (F); **d** The chamber-shaped thalli composed of *Korilophyton* (K) with possible *Lithocodium* (L) and growth pores represented by fenestral cavities (F). Both **c** and **d** demonstrate the possible *Bacinella* (B). Photomicrographs were taken under PPL

possibly filamentous networks that are filled by microspars. These aphanitic microtubules have diameters of 10–20 μm ("L" in Fig. 5c, d), and form an irregular-shaped mm-leveled tubular structure with relatively clear boundaries. For microproblematica that may be calcified cyanobacteria, there is continuing discussion regarding the biological affinity of *Lithocodium* than that of *Epiphyton*. One approach is to group these forms into a special sedimentary fabric that is marked by encrusting masses of irregular open micritic networks, e.g. the *Lithocodium*-like fabric rather than a possible microbial fossil (Rameil et al. 2010; Schlagintweit and Bover-Arnal 2013). Secondly, the "*Bacinella*-like" fabric as shown in Fig. 5c and d is microspar separated by thin films (~ 1 μm thick) of dark micrite which is relatively enriched in organic substances. These typical fabrics have been elucidated as microproblematica of the *Lithocodium*–*Bacinella* group (Cherchi and Schroeder 2006; Rameil et al. 2010; Schlagintweit and Bover-Arnal 2013), rather than a type of fossil calcimicrobe. Thirdly, special crystals of dolomites have the size of 10–20 μm with blurred core and clear rim (Fig. 5c). Although these crystals can be grouped into dolomitic cements (Choquette and Hiatt 2008) and/or dolomitic precipitates (Roberts et al. 2013), their genetic relationship with the dendrolites needs to be further investigated. Fourthly, the irregular-shaped mm-leveled fenestral cavities with clear boundaries ("F" in Fig. 5c, d) are observed. These fenestral cavities are filled with equant calcite spars forming granular and drusy mosaics without original pore space and obvious geopetal structures. Similar cavities have been observed in the cortex of Cambrian oncoids with abundant preserved fossils of filamentous cyanobacteria like *Girvanella* (Wilmeth et al. 2015; Riaz et al. 2020). These mm-

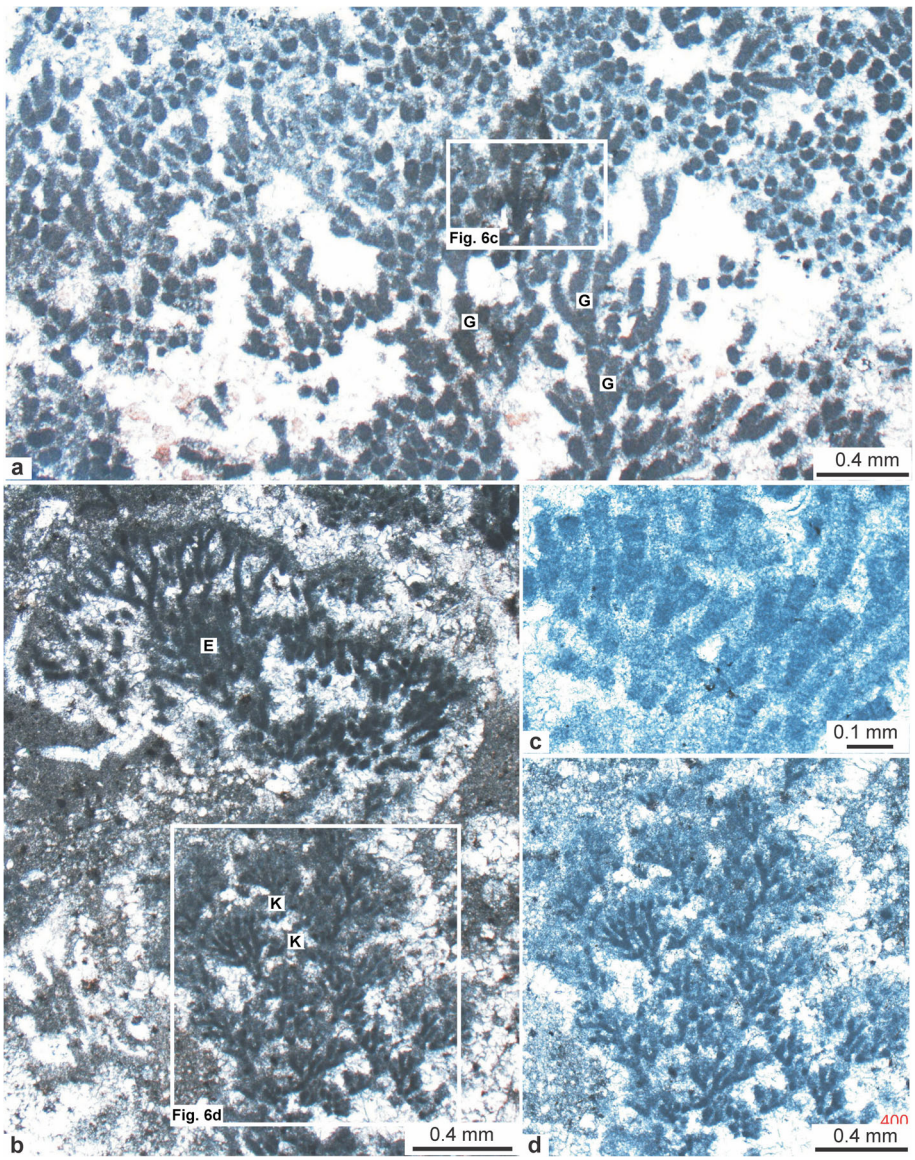

Fig. 6 Photomicrographs show the large-scale shrub-like thalli in the dendrolites in top part of the subsequence III of the Zhangxia Formation at the Anjiazhuang section, which are marked by the following phenomena: **a** Large-scale shrub-like thalli composed of *Gordonophyton* (G); **b** The development of large-scale shrub-like thalli respectively composed of typical *Epiphyton* (E) and *Korilophyton* (K); **c** Enlarged image of **a**, showing the *Gordonophyton* with the segmentation in solid micritic filaments that are 50–70 μm in diameter and 100–300 μm in length; **d** The enlargement of the *Korilophyton* ("K") in **b.** Photomicrographs were taken under PPL

scale fenestral cavities ("F" in Fig. 5c, d) may provide some useful information for further understanding of the forming process, especially the calcification of dendrolites.

Fossils of the possible calcimicrobes belong to the *Epiphyton* group in large-scale shrub-like thalli (Fig. 6), and can be further subdivided into three members (Riding 1991a, 1991b), that is: (1) the typical *Epiphyton* (solid micritic, dendritic) ("E" in Fig. 6b) consisting of bifurcating branches of dense micritic rods, 50–70 μm in diameter, which has been described as type I *Epiphyton* (Woo et al. 2008); (2) the *Gordonophyton* with segmentation (Fig. 6a, c), which is similar to typical *Epiphyton* in terms of outline thalli and branch dimension, and has been described as type II *Epiphyton* (Woo et al. 2008); and (3) the *Korilophyton* ("K" in Fig. 6b, d) with short branches and a large length-diameter ratio, which has been described as type III *Epiphyton* (Woo et al. 2008). Moreover, the special interstices within these large shrub-like thalli of *Epiphyton* are composed of carbonate spars that are different from the microscopic fabrics of possible *Lithocodium* ("B" in Fig. 5c, d) (Schlagintweit and Bover-

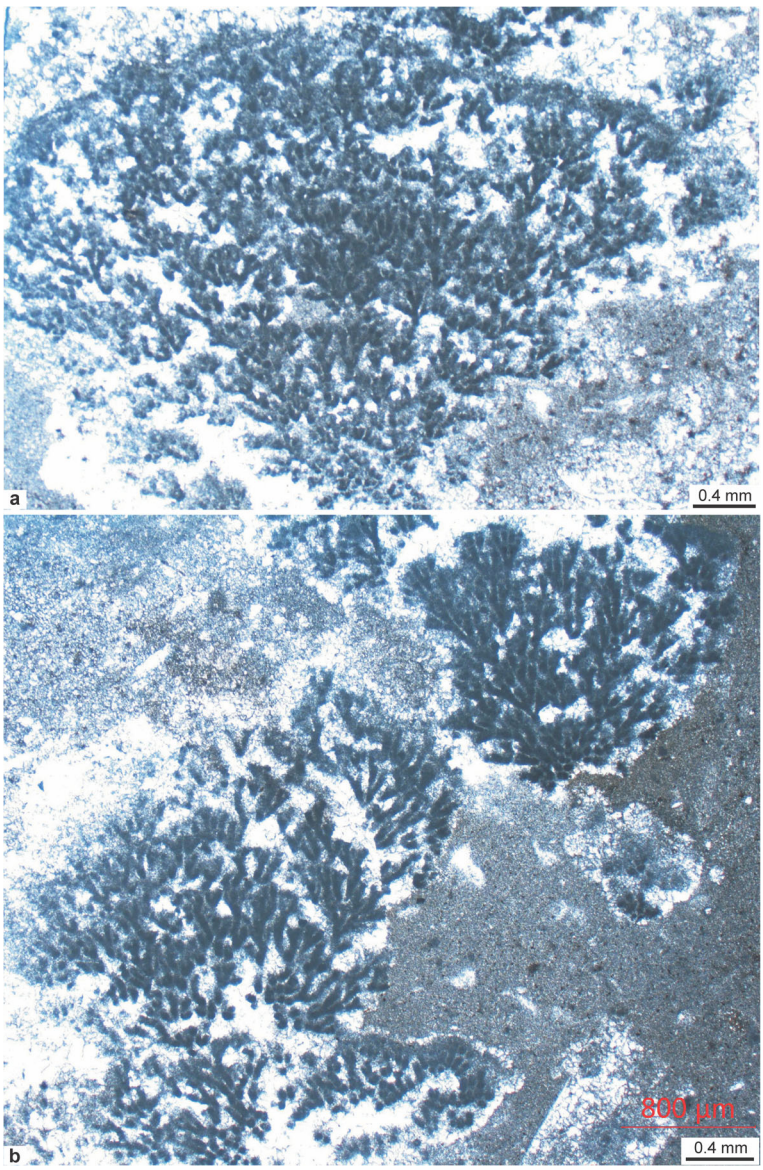

Fig. 7 Photomicrographs portray large-scale fan-like thalli of typical *Epiphyton* in the dendrolites in top part of the subsequence III of the Zhangxia Formation at the Anjiazhuang section, Shandong Province. **a** A cm-sized fan-shaped shrub-like thallus vegetates within the matrix represented by the *Bacinella*-like fabric; **b** Two cm-sized fan-shaped shrub-like thalli make an upgrowth in the transitional boundary between the matrix represented by the *Bacinella*-like fabric and the matrix composed of dense micrites with development of small-scale shrub-like thalli. Photomicrographs were taken under PPL

Arnal 2013). However, shrub-like thalli of *Epiphyton* are similar to filling carbonate spars of mm-scale fenestral cavities ("F" in Fig. 5c, d). Further, both *Epiphyton* and *Korilophyton* can develop the corresponding large-scale fan-shaped shrub-like thalli (Fig. 6b).

Moreover, possible calcimicrobe fossils of typical *Epiphyton* shape, with relatively thick bifurcating branches of dense micritic filaments, frequently vegetated into a cm-sized fan-shaped shrub-like thallus in the matrix represented by the "*Bacinella*-like" fabric (Rameil et al. 2010; Schlagintweit and Bover-Arnal 2013) (Fig. 7a). The fan-shaped shrub-like thalli develop in the transitional boundary between the matrix represented by the "*Bacinella*-like" fabric (Rameil et al. 2010; Schlagintweit and Bover-Arnal 2013) and dense micrites. The small shrub-like thalli can grow within dense micritic matrix (Fig. 7b). Furthermore, typical *Epiphyton* form large-scale (cm-sized) chamber-shaped colony (Fig. 8a, b) in the matrix composed of "*Bacinella*-like" fabric (Rameil et al. 2010; Schlagintweit and Bover-Arnal 2013). Several small-scale (< 1 mm) chamber-shaped colonies also vegetate in the matrix of the "*Bacinella*-like" fabric (Fig. 8c). These

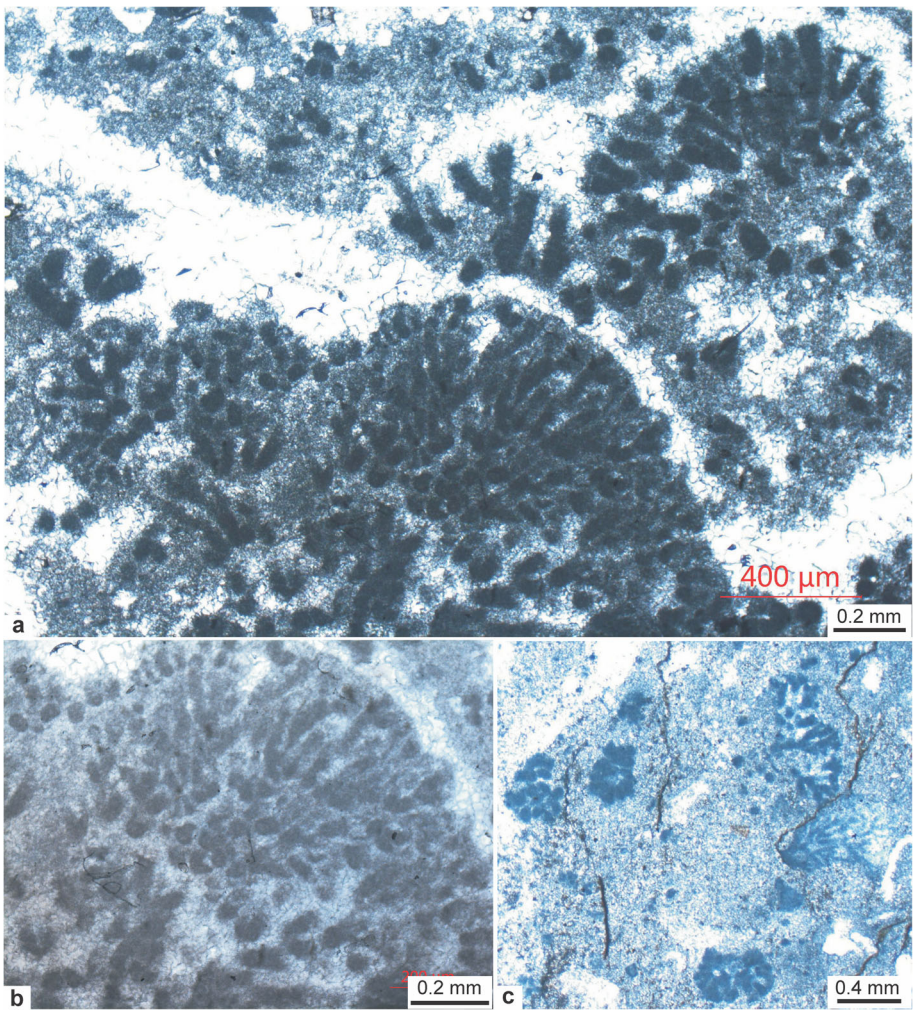

Fig. 8 Photomicrographs represent chamber-shaped colonies of *Epiphyton* within the dendrolites in top part of the subsequence III of the Zhangxia Formation at the Anjiazhuang section, Shandong Province. **a** A large-scale chamber-shaped colony composed of *Epiphyton*; **b** The enlarged image of the lower center of **a**; **c** Many small-scale chamber-shaped colonies composed of *Epiphyton* vegetating in the matrix of *Bacinella*-like fabric. Photomicrographs were taken under PPL

fossils of possible calcimicrobes belonging to *Korilophyton* with short branches and intergrowth of typical *Epiphyton* can also form large-scale bush-like colonies in the matrix of the "*Bacinella*-like" fabric (Rameil et al. 2010; Schlagintweit and Bover-Arnal 2013) (Fig. 9).

In the *Epiphyton* group, besides the above three members of typical *Epiphyton* (Figs. 5a, b, 6b, d, 7, 8), *Gordonophyton* (Fig. 6a, c), and *Korilophyton* (Figs. 6a, d, 9), *Hedstroemia* (Fig. 10), another typical fossil of calcified cyanobacteria is observed within the clotted clusters as shown in Fig. 4, which has been described as type IV *Epiphyton* (Woo et al. 2008). *Hedstroemia* is comprised of delicate tubular branched filaments characteristically arranged in fan-like radiating clusters, and is subdivided into two varieties: (1) typical *Hedstroemia* (Riding 1991b, 1991c; Woo et al. 2008; Yan et al. 2017) marked by a fan-like radiating cluster and is composed of relatively thick filaments (about 10 μm) ("H-1" in Fig. 10a); (2) the *Cayeuxia* (Riding 1991b, 1991c; Woo et al. 2008; Liu et al. 2016) that is characterized by a hemisphere-like radiating cluster, and is composed of relatively thin elongated filaments (< 5 μm) radiating from a base point ("H-2" in Fig. 10a, b, c). The colonies of typical *Hedstroemia* and *Cayeuxia* intergrow with the colony of *Epiphyton* (Fig. 10b). These colonies develop a microspar matrix composed of *Bacinella*-like fabric (Rameil et al. 2010; Schlagintweit and Bover-Arnal 2013), which further share following features: (a) branching clusters of tubes or filaments, (b) clusters with fan-like longitudinal section, (c) radial erect growth, and (d) adjacent tubes or filaments which either share common or separate walls.

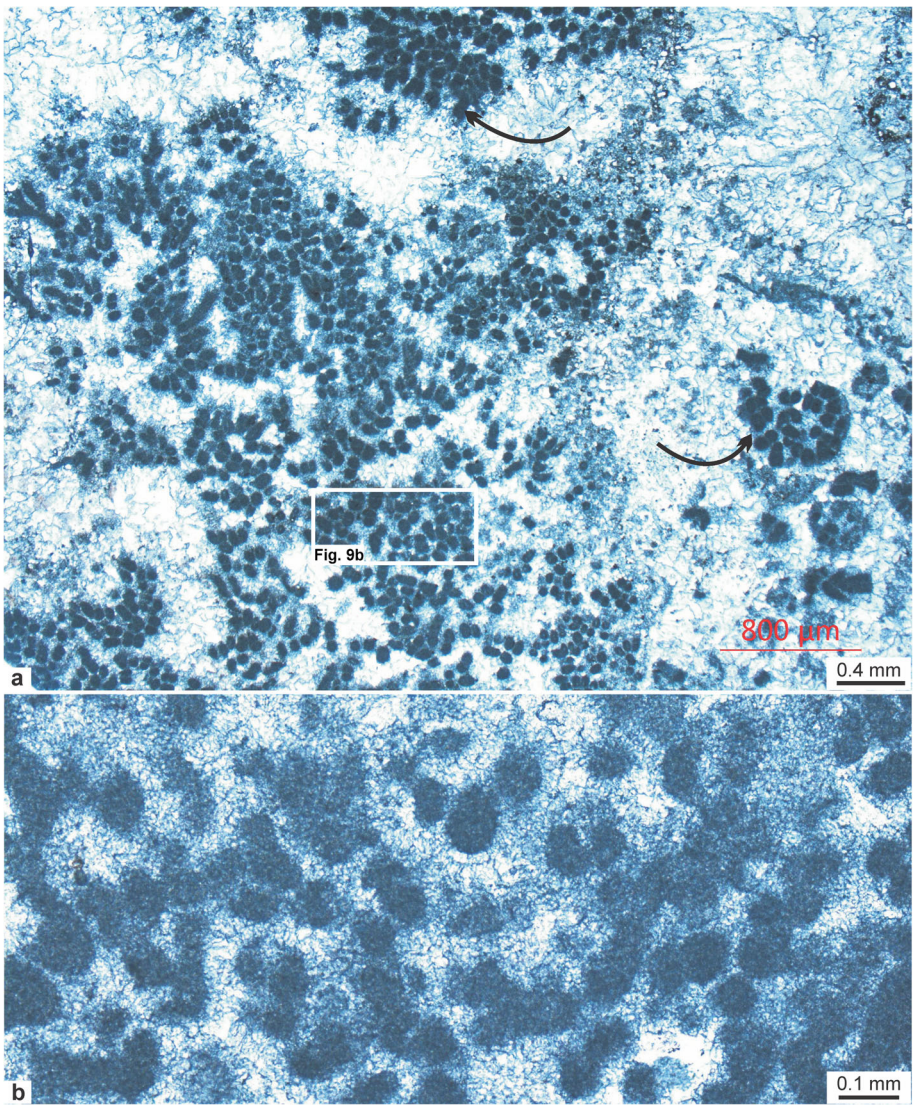

Fig. 9 Photomicrographs display large-scale bush-like colony of *Korilophyton* within dendrolite in top part of the subsequence III of the Zhangxia Formation at the Anjiazhuang section, Shandong Province. **a** A large-scale bush-like colony of *Korilophyton* with intergrowth of small colony of typical *Epiphyton* (arrows) within a matrix that is composed of *Bacinella*-like fabric; **b** Enlarged part of **a.** Photomicrographs were taken under PPL

4.2 Fundamental features of leiolite intergrown with dendrolite

4.2.1 Macroscopic feature

As mentioned above that isolated dendritic clusters of calcimicrobes are composed of mm- or cm-sized dark dense micrite (Fig. 4; e.g. Riding 1991a, 2000; Howell et al. 2011) which are similar to mesoclots in thrombolites (Aitken 1967), it led to the situation that dendrolite is commonly described as thrombolite (Kennard and James 1986; Woo and Chough 2010; Qi et al. 2014; Ezaki et al. 2017; Yan et al. 2017). In contrast, leiolite was regarded as a type of microbial carbonate (Braga et al. 1995) that is relatively structureless (aphanitic) with mesostructure, and lacking laminations and clots. It could be used as a synonym for "cryptomicrobialite" and could be grouped into thrombolite (Kennard and James 1986). No example of modern leiolite has been published (Dupraz et al. 2011), and only a few particular examples of ancient leiolites have been described in the stratigraphic record.

Some leiolites with intergrowth of dendrolites form massive limstones (Fig. 3d). These leiolites (Fig. 11) have no structure which fit to the definition of leiolite as described by Braga et al. (1995), Riding (1991a, 2000) and Dupraz et al. (2011). The macroscopic features of these leiolites are: (1) an abrupt boundary with dendrolites, which is a possible hardground; (2) the primary composition of dense micrites with a few small lenses or stripes

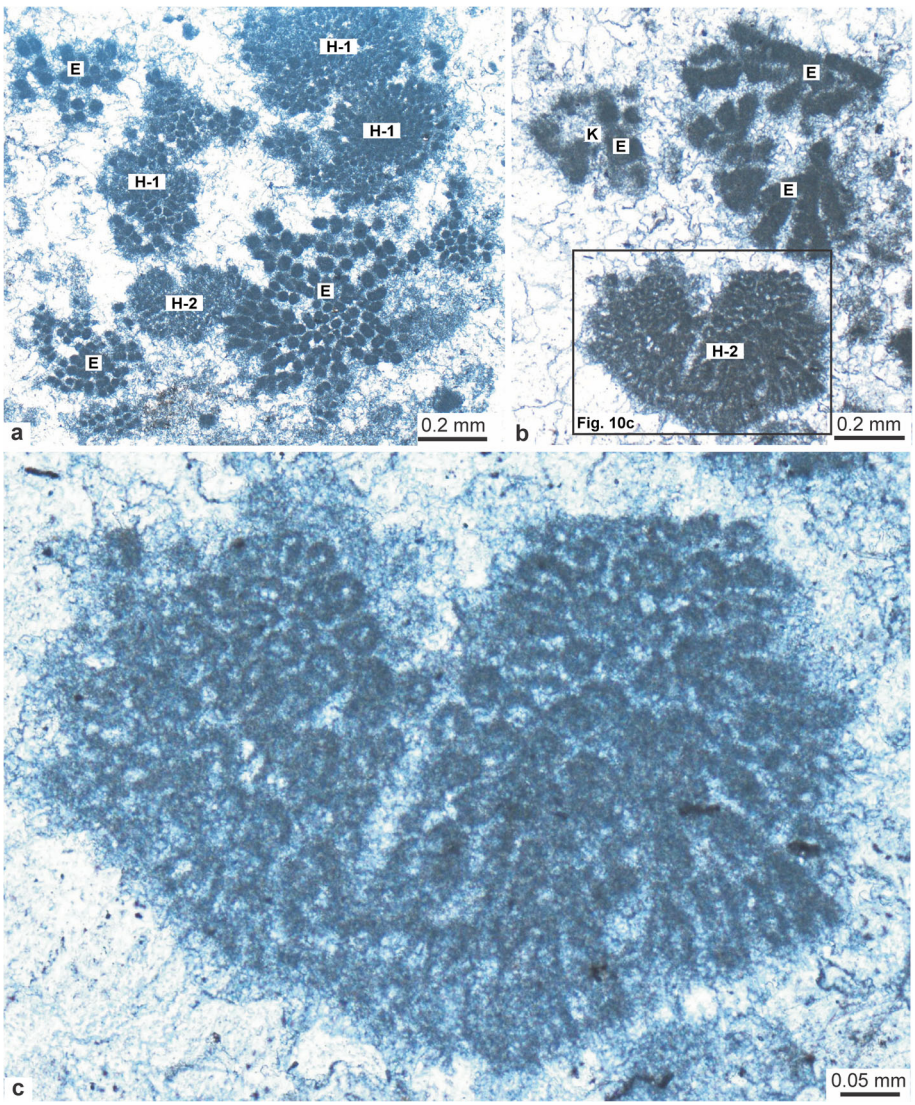

Fig. 10 Photomicrographs depict a *Hedstroemia* colony within dendrolite in top part of subsequence III of the Zhangxia Formation at the Anjiazhuang section, Shandong Province. **a, b** Intergrowth among colonies of typical *Hedstroemia* (H-1), *Cayeuxia* (H-2) and typical *Epiphyton* (E); **c** A typical *Cayeuxia* colony (enlarged in **b**). Photomicrographs were taken under PPL

of cherts (Fig. 11a, b); and (3) the possible heterogeneous sedimentary fabric comprising some irregular-shaped dark microclots (organic substances) and lenses of dolomite (Fig. 11c).

4.2.2 Microscopic feature

The leiolite of the Miaolingian Zhangxia Formation at the Anjiazhuang section provides distinctive characteristics of the heterogeneous sedimentary fabric (Fig. 12). As a fundamental feature of leiolite, the dense micrites (Fig. 12a) are partly rich in trilobite fossils (Fig. 12b). There are several other features of leiolite as below. (1) It shows a possible *Bacinella*-like fabric (Fig. 12c) which is similar to the fabric described in dendrolites (Figs. 5, 6, 7, 8, 9). (2) It contains occasional sponge fossils (Fig. 12d, e) with the outline of 6 mm in diameter and obvious spongocoel of about 2 mm in diameter. In term of the clear channel system and contrast to the *Lithocodium*-like fabric (Rameil et al. 2010; Schlagintweit and Bover-Arnal 2013) (Fig. 5c, d), the skeleton texture represented by regularly- and morphologically-repeated microspars in dense micrites, was grouped into the fossils of lithified sponge (Adachi et al. 2015; Lee et al. 2016). (3) There are small-scale (< 0.5 mm) colonies of *Epiphyton* within dense micritic fabrics (Fig. 12e).

The detailed observations show that microscopic fabrics of leiolites can be grouped into the special microspar fabric that is similar to *Bacinella* or *Bacinella*-like fabric (Rameil et al. 2010; Schlagintweit and Bover-Arnal 2013), and the dense micrites, which are associated with

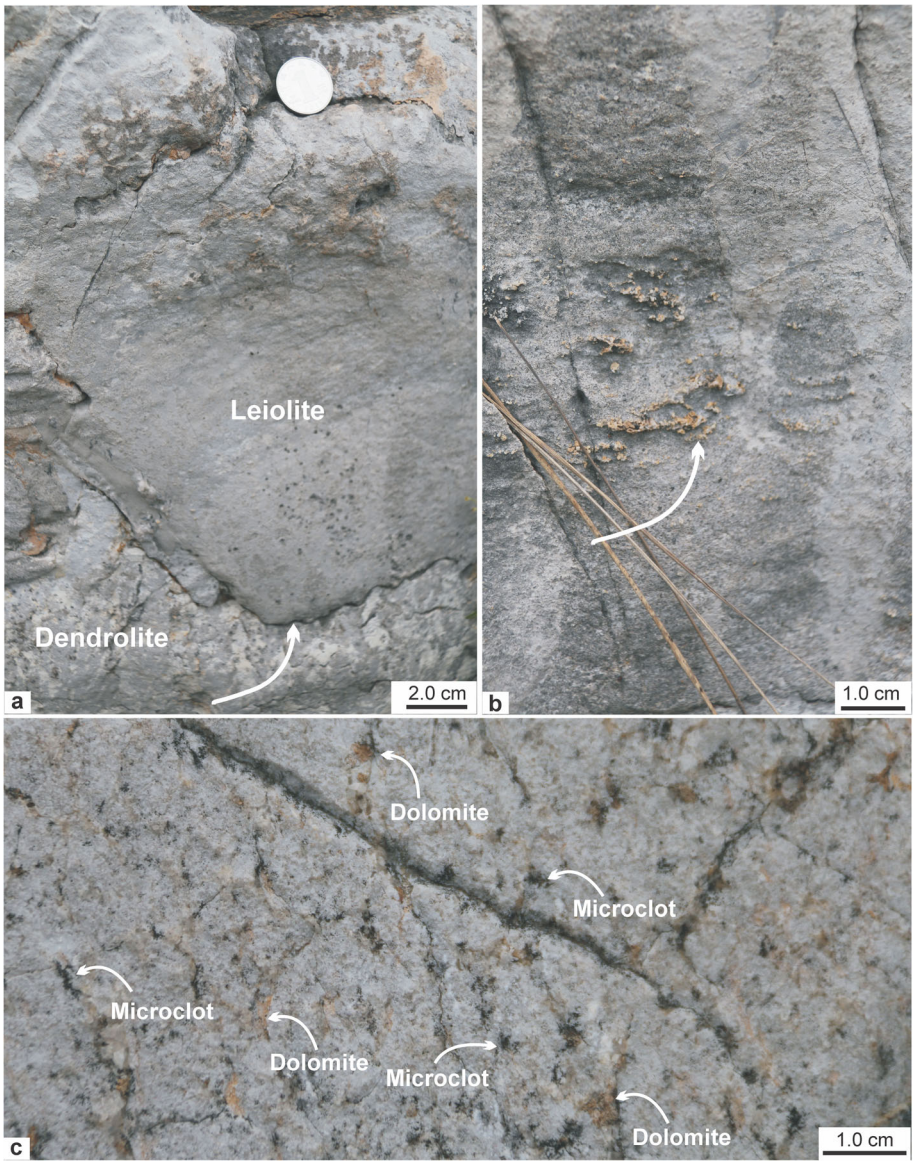

Fig. 11 Macroscopic photographs for the leiolite in top part of the subsequence III of the Zhangxia Formation at the Anjiazhuang section, Shandong Province. **a** A large-scale len-shaped leiolite within dendrolite. The boundary (arrow) between the leiolite and the dendrolite is a possible hardground; **b** The structureless leiolite contains micrite and some chert (arrow); **c** Possible heterogenous fabric comprising of some irregular-shaped dark microclots and brown lens of dolomite

many small-scale colonies of mm-sized *Epiphyton* as well as other fossils of calcimicrobes (Fig. 13). Some possible calcimicrobes observed in dense micrites belong to *Renalcis* (Fig. 13c), which have clusters of hollow reniform bodies with a diameter of 50–100 μm, and have thick walls of micrite. Some ambiguous and non-tangled fossils of calcified filamentous cyanobacteria which have a length of several hundreds micrometers and a diameter of 10–20 μm are identified in transitional boundary between the dense micritic fabric and the "*Bacinella*-like" fabric (Fig. 13d, e). The slightly even walls (1–2 μm in thickness) of calcified fossils of filamentous cyanobacteria are composed of dark micrites and are comparable to modern *Tychonema* (De los Ríos et al. 2015). It can be grouped into a new type of fossil, i.e. the *Girvanella* group (Riding 1991b, 1991c).

Typical and tangled filamentous fossils of *Girvanella* intergrowing with small-scale (about 0.1 mm) colonies of *Epiphyton* were observed inside *Bacinella*-like fabric (Fig. 14). These filamentous fossils are several hundreds of micrometers in length, about 10 μm in diameter, and with a dark micritic wall in thickness of 1–2 μm (Fig. 14b, c). Like non-tangled fossils of calcified filamentous cyanobacteria (Fig. 13d, e), the relatively even walls of

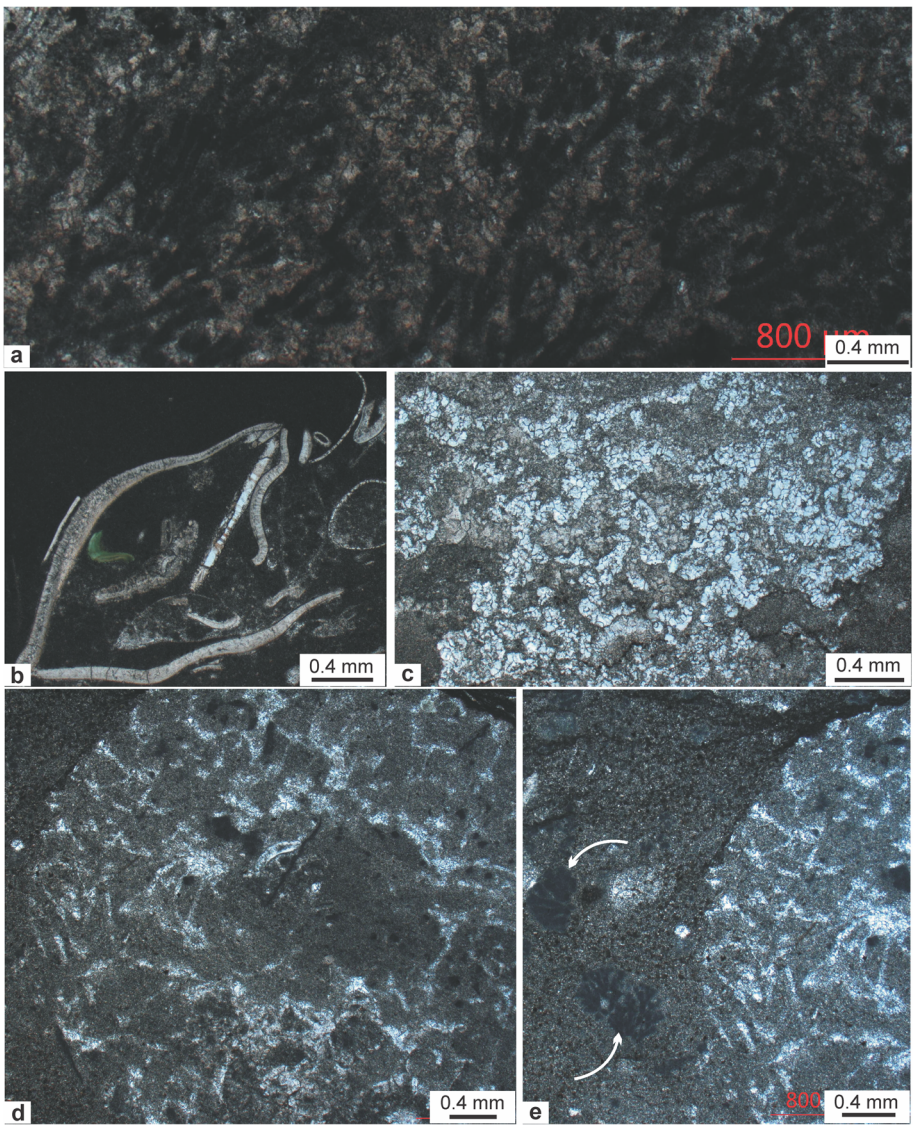

Fig. 12 Photomicrographs of leiolite in top part of the subsequence III of the Zhangxia Formation at the Anjiazhuang section, Shandong Province. **a** Dense micrites of leiolite; **b** Trilobite fossils within dense micrites of leiolite; **c** Possible *Bacinella*-like fabric within the leiolite; **d** A possible sponge fossil; **e** Small-scale conolies of *Epiphyton* (arrows) and a part of a sponge fossil (the right) within dense micrites of the leiolite. Photomicrographs were taken under PPL

tangled fossils may be products of in vivo calcification, which is genetically related to ecophysiological concentration of atmospheric CO_2 (Kah and Riding 2007) and is beyond the scope of present study. Furthermore, they are grouped into typical fossils of *Girvanella* and are similar to modern *Plectonema* (Riding 1991b, 1991c).

Further observation indicates that the *Lithocodium*- and *Bacinella*-like fabrics are the fundamental fabrics for the leiolite (transitional type between leiolite and dendrolite) (Fig. 15a, b). The *Lithocodium*-like fabric may intergrow with the *Bacinella*-like fabric (Fig. 15a), or isolatedly occur within the *Bacinella*-like fabric (Fig. 15b). Importantly, small (200–400 μm) chamber-like or irregular-shaped colonies of *Epiphyton* not only overgrow within the *Lithocodium*-like fabric (Fig. 15a–d) but also occur in the *Bacinella*-like fabric (Figs. 15a and 16). The phenamenon further demonstrates that the *Lithocodium*- and *Bacinella*-like fabrics can be used as growth matrix of small colonies of *Epiphyton*, which is similar to the phenomenon of the Late Jurassic *Epiphyton*-like cyanobacteria described by Săsăran et al. (2014).

5 Discussion

Microbial reefs with a thickness of more than 100 m are observed in upper part of subsequence III of the Miaolingian Zhangxia Formation at the Anjiazhuang section

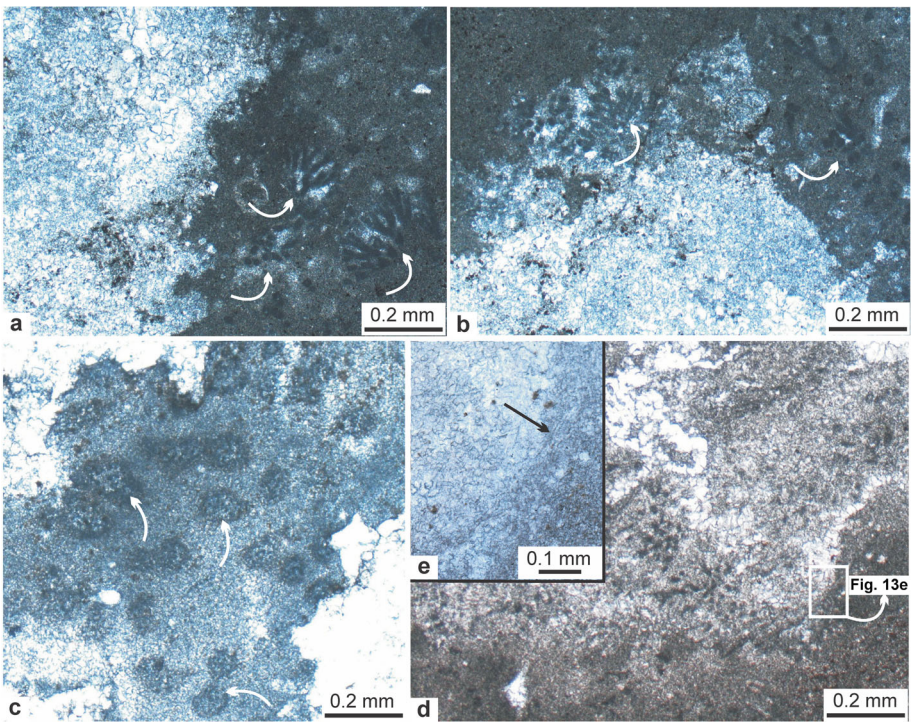

Fig. 13 Photomicrographs show the fossils of calcified cyanobacteria within leiolite in top part of the subsequence III of the Zhangxia Formation at the Anjiazhuang section, Shandong Province. **a** Possible *Bacinella* (or *Bacinella*-like fabric; the left part), and many small-scale colonies of *Epiphyton* (arrows) within dense micrites of leiolite (the right part); **b** Possible *Bacinella* (the lower part), and many small-scale colonies of *Epiphyton* (arrows) within dense micrites of the leiolite (the upper part) and in the transitional zone; **c** Some possible fossils of *Renalcid* (arrows); **d** Intergrowth of *Bacinella*-like fabric (the upper part) and the dense micritic fabric (the lower part); **e** Enlarged part of **d** shows some obscure fossils of calcified filamentous cyanobacteria (arrow) in the transitional boundary of the two fabrics. Photomicrographs were taken under PPL

in Feicheng city of Shandong Province (Figs. 1, 2b and 3). They are dominated by dendrolites with intergrowth of leiolites, and were formed during the forced regression period that fulfills the model of Hunt and Tucker (1992), Mei and Yang (2000), and Schlager and Warrlich (2009). The Zhangxia Formation is a third-order sequence bounded by "drowning unconformities" (e.g. Schlager 1989, 1998, 1999), which represents a macroscopically remarkable sedimentary deposit and conforms to the concept of microbial reef that is formed in a relatively high-energy marine environment (Riding 2002a; Rowland and Shapiro 2002; Kiessling 2009; Lee et al. 2014a, 2014b, 2015, 2019; Lee and Riding 2018; Cordie et al. 2019).

The dendrolites are made up of cm- and mm-sized dark dense micritic clots which are bush-like (or shrubs) (Fig. 4). These clots are macroscopically similar to the mesoclots inside the thrombolites (Aitken 1967; Kennard and James 1986). However, they have different possible calcimicrobes, i.e. the *Epiphyton* group, including typical *Epiphyton* (Figs. 5a, b, 6b, d, 7 and 8), the *Gordonophyton* (Fig. 6a, c), and the *Korilophyton* (Figs. 6b, d and 9), which make the Miaolingian dendrolites structurally distinct from the clotted thrombolites (Riding 1991a, 2000; Howell et al. 2011). Therefore, diversified calcimicrobes and complicated sedimentary fabrics of Miaolingain dendrolites at a microscopic level, are relatively more sophisticated than previously visualized.

The typical inference of calcified fossils of the *Epiphyton* group (Figs. 5, 6, 7, 8, 9) in clotted clusters (Fig. 4) can be an analogue to modern cyanobacteria such as *Stigonema* (Riding 1991b, 1991c; Laval et al. 2000; Woo et al. 2008; Woo and Chough 2010; Ezaki et al. 2017; Mei et al. 2017, 2020), which further reflect the following phenomena: (1) possible modern analogue of shrub fabric in the Miaolingian dendrolites was formed by typical filamenteous cyanobacteria (Laval et al. 2000; Bradley et al. 2017); and (2) possible calcified fossils, i.e. the *Gordonophyton* (Fig. 6a, c), are similar to modern cyanobacteria such as *Lyngbya* or *Tolypothrix* that form hormogonia (Mohr et al. 2011; Suosaari et al. 2018). The present paper follows this typical idea. There are different thoughts for the biological affinity of fossils belonging to *Epiphyton* group (Figs. 5, 6, 7, 8, 9, 10, 12, 13, 14), such as: (1) evolution in life cycle similar to calcareous red algae (Luchinina and Terleev 2008, 2014; Luchinina 2009); (2) precipitation via bacteria rather than photosynthetic cyanobacteria (Chafetz and Guidry 1999); (3) a

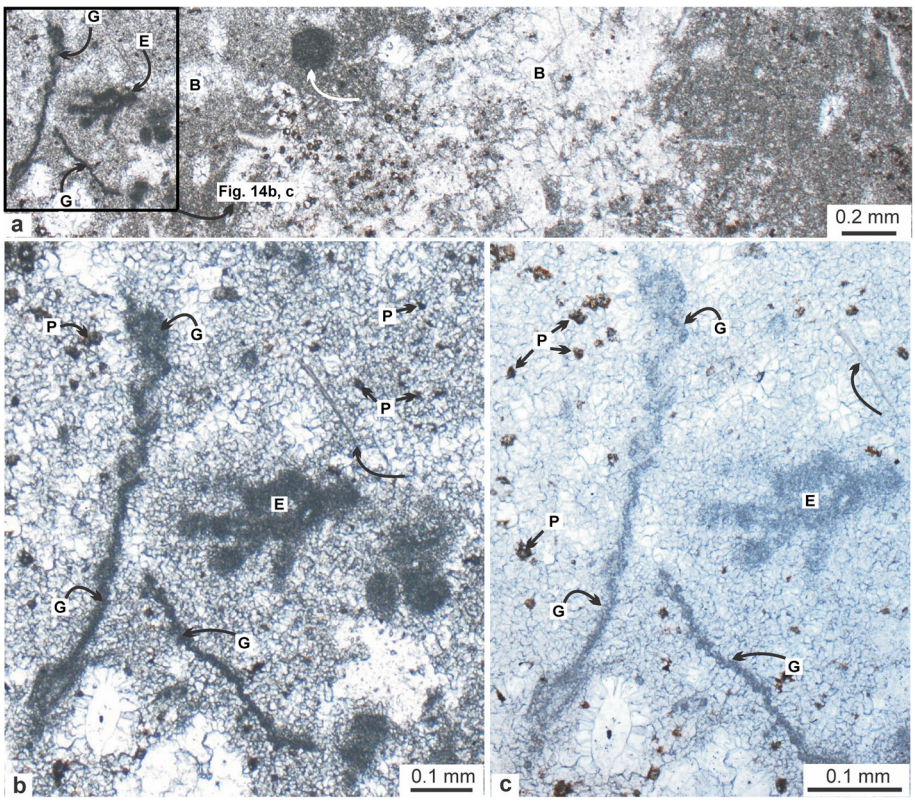

Fig. 14 Photomicrographs display *Girvanella* that is paragenetic with small chamber-like colonies of *Epiphyton* within the leiolite in top part of the subsequence III of the Zhangxia Formation at the Anjiazhuang section, Shandong Province. **a** Interclated intergrowth of the *Bacinella*-like fabric (B) and the dense micritic fabric with a possible microburrow (white arrow), as well as intergrowth of the *Epiphyton* (E) and the *Girvanella* (G; strip-like bodies of dense micrites) under low resolution; **b**, **c** Enlarged part of **a** showing an obvious filamentous fossil of *Girvanella* (G). The *Girvanella* are aggregated into bundles like the *Subtifloria*, which however, are distinctly different when compare the *Subtifloria* with present-day *Microcoleus*, a special type of *Girvanella* of highly tangled filaments. The black dots within **b** and **c** might be residues of pyrites (P). Photomicrographs were taken under PPL

type of microbial fossil that can not be grouped into calcified cyanobacteria like *Renalcis* (Adachi et al. 2014); and (4) calcified microproblematica (Liu et al. 2016). Furthermore, phototropism of *Epiphyton* (Woo and Chough 2010) provides relatively more reasonable explanation for their recognition through following phenomena: (a) the intergrowth of *Epiphyton* and *Hedstroemia* within the dendrolites is shown in Fig. 11, with the *Hedstroemia* analogue to modern cyanobacteria *Rivularia* (Whitton and Mateo 2012; Liu et al. 2016; Mlewski et al. 2018); and (b) the intergrowth of *Epiphyton* and *Girvanella* in leiolites is shown in Figs. 13e and 14, with *Girvanella* similar to modern cyanobacteria *Plectonema* or *Tychonema* (Riding 1991b, 1991c; De los Ríos et al. 2015). Therefore, based on cyanobacterial affinity of *Epiphyton*, it is assumed that shrubs in the Miaolingian dendrolites are constructed by filamentous cyanobacteria like the modern examples (Bradley et al. 2017; Suosaari et al. 2018).

However, two fabrics of possible calcimicrobes increase complexity for the dendrolites in this study, i.e., (1) the possible *Lithocodium* or *Lithocodium*-like fabric (Cherchi and Schroeder 2006; Rameil et al. 2010; Schlagintweit and Bover-Arnal 2013) which comprise micritic aggregation with filamentous networks or aphanitic–microtubular fabric within dark dense micrites of the dendrolites ("L" in Fig. 5c, d) and the leiolites ("L" in Fig. 15); (2) *Bacinella* or *Bacinella*-like fabric (Rameil et al. 2010; Schlagintweit and Bover-Arnal 2013) in the dendrolites (Figs. 5, 6, 7, 8, 9, 10) and the leiolites (Figs. 11 and 13 to 14, 15a, b and 16) which is marked by microscopic fabrics that are separated by thin films of dark micrites. Although they make up a possible group of calcified cyanobacteria, i.e. the *Lithocodium–Bacinella* group (Riding 1991b, 1991c), with more uncertainties and strong disputations, the *Lithocodium*-like fabric (Rameil et al. 2010) has been a form of codiacean algae by nomenclature (Elliott 1956) and was interpreted as a type of foraminifer (Schmid and Leinfelder 1996). Therefore, it is suggested that this fabric should be grouped into possible residue of colonies of calcified cyanobacteria (Cherchi and Schroeder 2006) or micro-encrusters

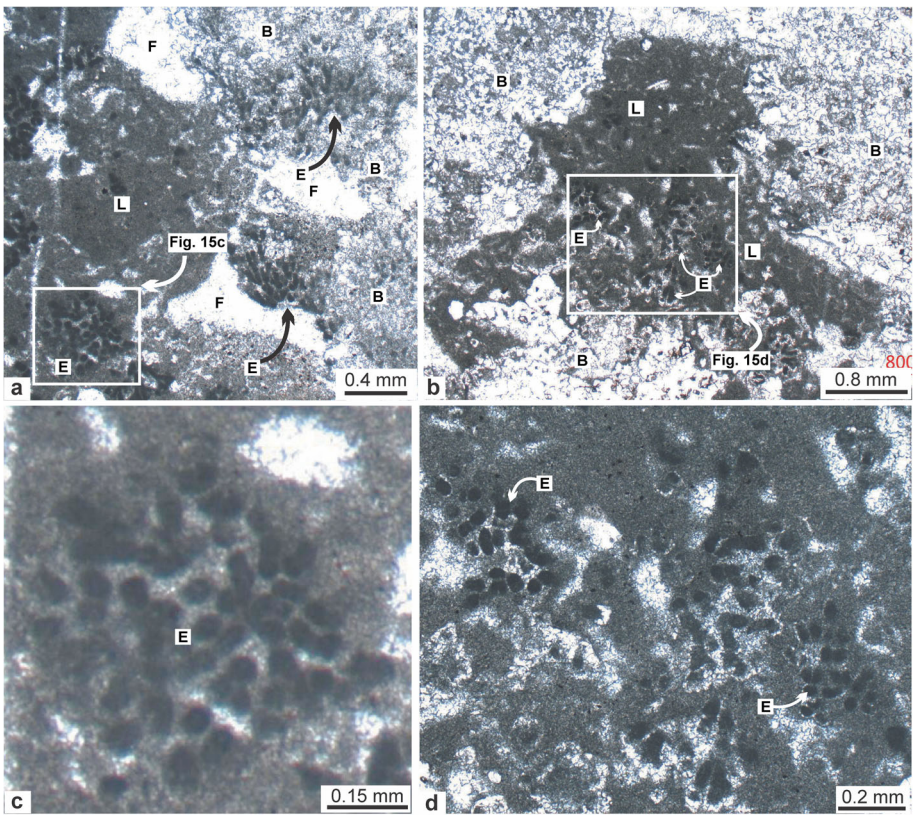

Fig. 15 Photomicrographs show the intergrowth between *Lithocodium*-like and possible *Bacinella*-like fabrics with the overgrowth of small chamber-like or irregular-shaped colonies of *Epiphyton* within the leiolite in top part of the subsequence III of the Zhangxia Formation at the Anjiazhuang section, Shandong Province. **a** Intergrowth between the *Lithocodium*-like (L) and the possible *Bacinella*-like (B) fabrics with some fenestral cavities filled by carbonate spars (F) and overgrowth of colonies of *Epiphyton* (E); **b** Isolated *Lithocodium*-like fabric (L) and the overgrowth colonies of *Epiphyton* (E) within the *Bacinella*-like fabric (B); **c** Overgrowth of small chamber-like colonies of *Epiphyton* (E) within *Lithocodium*-like fabric (zoomed in **a**); **d** Overgrowth colonies of *Epiphyton* (E) within the *Lithocodium*-like fabric (zoomed in **b**). Photomicrographs were taken under PPL

that may suggest a phototrophic metabolism (Rameil et al. 2010). Although the *Bacinella*-like fabric (Schlagintweit and Bover-Arnal 2013) was interpreted as a type of algae in nomenclature (Radoičić 1959) and later interpreted as a type of green algae (Schlagintweit et al. 2010), further research suggested that the *Bacinella*-like fabric should be grouped into a feature of modern microbialites (e.g., microbial mats) (Schlagintweit and Bover-Arnal 2013). As a possible group of calcified cyanobacteria, the *Lithocodium–Bacinella* group (Riding 1991b, 1991c) has been widely described in microbial carbonates of the Mesozoic (Cherchi and Schroeder 2006; Védrine et al. 2007; Rameil et al. 2010; Schlagintweit and Bover-Arnal 2013). Futhermore, the *Lithocodium* or the *Lithocodium*-like fabric is enigmatically similar to sedimentary fabric (Figs. 5c and 15), which has been frequently interpreted as sponge cast in recent years, i.e., (1) the network of spicules of silicious sponge (Kwon et al. 2012; Chen et al. 2014a, 2014b; Lee et al. 2014a, 2014b, 2015; Li et al. 2015; Park et al. 2015; Coulson and Brand 2016; Shen and Neuweiler 2018), and (2) the sponge fibre of non-spicular keratose demosponges (Luo and Reitner 2014, 2016; Larmagnat and Neuweiler 2015; Lee and Riding 2018; Shen and Neuweiler 2018; Lee et al. 2019). All of these increase complexity for biological affinity of the "*Lithocodium*-like" fabric (Rameil et al. 2010; Schlagintweit and Bover-Arnal 2013). However, true sponge fossils composed of spicules (Fig. 12d, e) are distinctive from the "*Lithocodium*-like" fabric represented by microsparic microcanaliculus in the dense dark micrites (Figs. 5c, d and 15) (Rameil et al. 2010; Schlagintweit and Bover-Arnal 2013). Further, it provides some useful information to interpret the *Lithocodium* or the *Lithocodium*-like fabric as a colony of calcified cyanobacteria (Cherchi and Schroeder 2006) and a useful mirror image for studies of many researchers who always interpreted it as a spongy cast in recent years (Kwon et al. 2012; Chen et al. 2014a, 2014b; Lee et al. 2014a, 2014b, 2015; Li et al. 2015; Luo and Reitner 2014, 2016; Larmagnat and Neuweiler 2015;

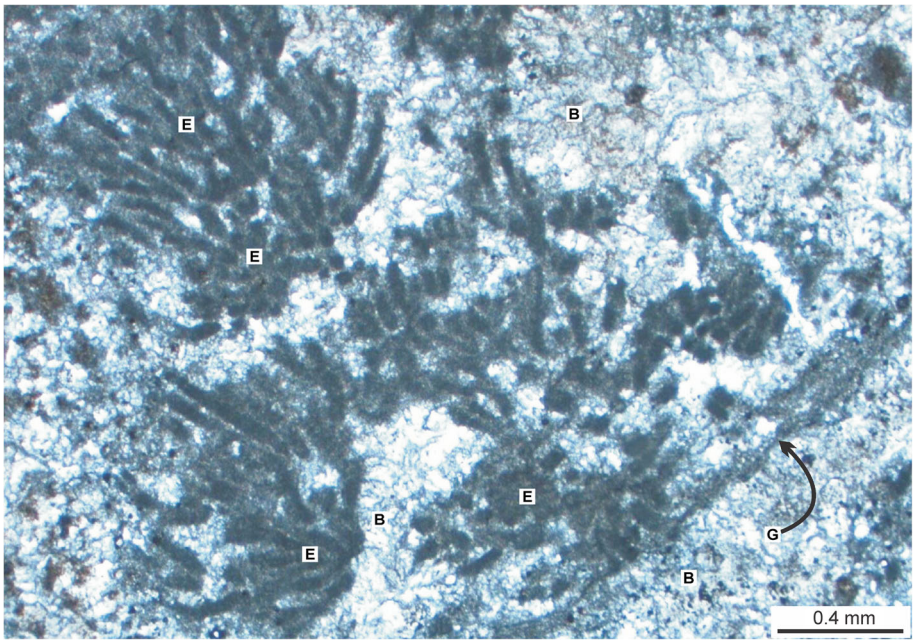

Fig. 16 Photomicrograph displays the overgrowth of small colonies of *Epiphyton* (E) and possible fossils of *Girvanella* (G) within the possible *Bacinella*-like fabric (B) in top part of the subsequence III of the Zhangxia Formation at the Anjiazhuang section, Shandong Province. Photomicrograph was taken under PPL

Park et al. 2015; Coulson and Brand 2016; Lee and Riding 2018; Shen and Neuweiler 2018; Lee et al. 2019). Futhermore, the establishment of the *Lithocodium* or *Lithocodium*-like fabric within Miaolingian dendrolites and leiolites may provide some useful thinking approaches and a research clue for further research of the history of Early Paleozoic skeletal reefs (Rowland and Shapiro 2002; Kiessling 2009; Lee et al. 2015, 2019; Ezaki et al. 2017; Lee and Riding 2018; Cordie et al. 2019), microbe-metazoan transitions of the Cambrian (Chen et al. 2019) and their driving factors (Rowland and Shapiro 2002; Kiessling 2009; Lee and Riding 2018; Riding et al. 2019). For example, the Cambrian/mid-Ordovician (541–465 Ma) is a period marked by abundance of microbial carbonate (MC) (Riding et al. 2019) and overall lack of metazoan reef-framework builders (Rowland and Shapiro 2002; Kiessling 2009; McKenzie et al. 2014; Ezaki et al. 2017; Cordie et al. 2019). Further dominant lithisted sponge–microbial reefs are documented during the Miaolingian to the Furongian (Chen et al. 2014b; Lee et al. 2015, 2019; Lee and Riding 2018; Cordie et al. 2019) and the peak of metazoa are marked by maceriate (maze-like) sponge reef during the late Furongian (Chen et al. 2019), which can not support actual microbial components like *Lithocodium* or *Lithocodium*-like fabric during the Cambrian (Figs. 5c, d and 15).

On the basis of two important cognitions, i.e. the *Lithocodium* or *Lithocodium*-like fabric should be grouped into a colony of calcified cyanobacteria (Cherchi and Schroeder 2006), and a micro-encruster might suggest a phototrophic metabolism (Rameil et al. 2010), it is more reasonable to imagine that *Lithocodium*-like fabric (Figs. 5c, d and 15) should be resulted from the calcification of one type of filamentous cyanobacteria with common sheaths, i.e. the *Nostoc* (Potts 1997; Wright et al. 2005; Soule et al. 2009; Helm and Potts 2012). Although this idea is a bold interpretation that needs further investigation, some of their evidence is as follows. (1) Similar to the dark micrites forming wall of calcified cyanobacteria like the *Girvanella* (Figs. 13e and 14), it might be resulted from in vivo calcification of structured sheaths (Riding 1991b, 1991c, 2011b; Kah and Riding 2007) composed of extracellular polymeric substances (EPSs; Dupraz et al. 2009, 2011; Decho 2010, 2011; Stal 2012; Tourney and Ngwenya 2014; Decho and Gutierrez 2017) with special protein of extracellular sunscreen scytonemins. Similarly, dark dense micritic matrix which hosted the aphanitic–microtubular fabric of the *Lithocodium*-like fabric (Figs. 5c, d and 15) might result from in vivo calcification of structured common sheath of *Nostoc* that is made up of EPS along with extracellular sunscreen scytonemin (Potts 1997; Wright et al. 2005; Soule et al. 2009; Helm and Potts 2012). (2) Irregular and snaky filaments of aphanitic–microtubulars with diameter of 10–20 μm are filled by microspars within dark dense micrites ("L" in Figs. 5c, d and 15). They might be a decomposition residue of the filaments (trichomes) of *Nostoc*, which are similar to the calcified

residue of filamentous cyanobacteria like the *Girvanella* that are mimic to the modern cyanobacteria *Plectonema* or *Tychonema* (Riding 1991b, 1991c; De los Ríos et al. 2015) (Figs. 13e and 14).

The intergrowth among the *Bacinella*-like fabric (Fig. 6c, d) (Riding 1991b, 1991c; Cherchi and Schroeder 2006; Védrine et al. 2007; Schlagintweit and Bover-Arnal 2013), *Lithocodium*-like fabric (Rameil et al. 2010; Schlagintweit and Bover-Arnal 2013), and *Epiphyton* in the dendrolites (Fig. 6c, d) and the leiolites (Figs. 15a, b and 16) clearly demonstrates that the *Lithocodium*-like fabric should be grouped into a type of microbial crusts. Finally, the *Lithocodium*-like fabric (Figs. 6c, d, 15 and 16) can be an analogue to modern *Nostoc* colonies with grape-shape or irregular morphology, and the size ranges from several tens to hundreds micrometers within microbial mats dominated by filamenteous cyanobacteria (De los Ríos et al. 2015). However, there are lots of detailed problems that need further research.

Microbial reefs dominated by dendrolites with intergrowth of leiolites in the Miaolingian Zhangxia Formation at the Anjiazhuang section (Fig. 3) depicted sophisticated calcification on microbial mats comprised of cyanobacteria (Stal 2012), including: (1) the intergrowth of multiple cyanobacterial colonies in the dendrolites such as possible *Nostoc* (Potts 1997; Wright et al. 2005; Soule et al. 2009; Helm and Potts 2012) (Fig. 5c, d), the *Epiphyton* (Figs. 5, 6, 7, 8, 9, 10), and *Hedstroemia* (Fig. 10); (2) sheath of filamentous calcified cyanobacteria such as *Girvanella* within the leiolites (Figs. 13e, 14 and 16); 3) widespread *Bacinella*-like fabric in the dendrolites (Figs. 5, 6, 7, 8, 9, 10, 11) and the leiolites (Figs. 14, 15, 16) that forms a special matrix for the growth of multiple colonies of cyanobacteria. Like the modern analogies of dendrolites, which are dominated by filamentous cyanobacteria that forming dendritic microstructure (Laval et al. 2000), dendrolitic cone (Bradley et al. 2017), and dendrolitic shrub (Suosaari et al. 2018), the clotted clusters are composed of dark dense micrites (Fig. 4) which can be interpreted as shrubs that are chiefly dominated by *Epiphyton* (Figs. 5, 6, 7, 8, 9) and *Hedstroemia* (Fig. 10). They occurred on an underlying microbial mat (Figs. 5, 6, 7, 8, 9) that is represented by *Bacinella*-like fabric, which can be grouped into a feature of modern microbialites (e.g. microbial mats) (Schlagintweit and Bover-Arnal 2013). The dense micrite may be understood as the result of precipitation of $CaCO_3$ morphs occurred simultaneously in metabolically active cyanobacterial layers (Kaźmierczak et al. 2015). It should be noted that widespread *Bacinella*-like fabric in the dendrolites (Figs. 5, 6, 7, 8, 9, 10, 11) and the leiolites (Figs. 14, 15, 16) are not completely similar to the typical *Bacinella*-like fabric of the Lower Aptian (Schlagintweit and Bover-Arnal 2013). However, following features can still characterize this type of fabric as an irregular vesicular microcrust that follows some of the formative characteristics of microbialites: (1) a distinctive growth matrix of multiple colonies of cyanobacteria from the dense micrites; (2) a spiecial composition of microspars that are separated by thin films (~ 1 μm) of dark micrites enriched with relatively more organic substances that are distinctive from common inorganic micrites or microspars; and (3) the diversified calcified microbes especially for those fossils of calcified sheath of cyanobacteria represent by *Girvanella*, possible *Nostoc* and *Epiphyton* within this type of fabric. Further investigations required on their ultramicrofabric characteristics and microorganisms that involved in their formation, can lead to a result of true sedimentary and microbial nature of this type of enigamatic fabric.

Of course, it can not simply think that the microbial reefs in the Miaolingian Zhangxia Formation (Fig. 3) are the products directly built up by cyanobacteria. It is definitely a result of complicated microbial precipitation (Riding 2000, 2011b) or the early lithification (Dupraz et al. 2009, 2011) in the microbial mats dominated by cyanobacteria. However, a major problem is the fact that majority of present day microbial mats dominated by cyanobacteria do not form consolidated rocks (Stal 2012). Further, these dendrolites (Figs. 3, 4, 5, 6, 7, 8, 9) with intergrowth of leiolites (Figs. 11, 12, 13, 14) may be products of sophisticated calcification of EPS (Dupraz et al. 2009, 2011; Decho 2010, 2011; Stal 2012; Tourney and Ngwenya 2014; De los Ríos et al. 2015; Decho and Gutierrez 2017) that form microbial biofilms (Riding 2000, 2002b; Flemming and Wingender 2010; Reitner 2011a; Flemming et al. 2016) in microbial mats (Gerdes 2010; Mei 2011b, 2014; Reitner 2011b) dominated by cyanobacteria. Although there are lots of problems needing future investigation, these dendrolites (Figs. 3, 4, 5, 6, 7, 8, 9) with the intergrowth of leiolites (Figs. 11, 12, 13, 14, 15, 16) occur as consolidated rocks, and show a complex mineral composition, including: (1) chert lenses in the leiolites (Fig. 11b), (2) special dolomitic cement in the dendrolites (Fig. 5c), and (3) residue of pyrite inside the dendrolites (Figs. 6, 7, 8, 9) and the leiolites (Fig. 14).

The dolomitic cement (e.g. Choquette and Hiatt 2008) in the dendrolites (Fig. 5c) may be classified into a dolomitic precipitate formed in the microenvironment enriched with organic substances in microbial mat (or biofilm) (Roberts et al. 2013; Gregg et al. 2015). In addition, it might represent the residue resulting from organic mineralization of amorphous magnesium silicate before the calcification of EPS making up microbial mats (or biofilms) (Miller and James 2012; Pacton et al. 2012; Burne et al. 2014; Perri et al. 2018). Further, this type of residue not only represents a particular organic dolomite (Mazzullo 2000; Mei 2012) but also forms a special

dolomitic residue (including the chert) in microbial carbonates (Kruse and Reitner 2014) like dendrolite as shown in Fig. 5c. Thus, the small-scale chert lenses (Fig. 11b) might be products of similar process.

The possible pyrite residues in dendrolites (Figs. 6, 7, 8) and leiolites (Fig. 14) might be a result of microbial precipitation (Riding 2000, 2011b) or early lithification (Dupraz et al. 2009, 2011), genetically related to sulfate reduction (Rickard et al. 2017; Lin et al. 2018; Bostick 2019). It also demonstrates two key components i.e. the alkalinity engine (Gallagher et al. 2012) and the organic EPS matrix (Decho 2010; Flemming and Wingender 2010; Tourney and Ngwenya 2014; Flemming et al. 2016; Decho and Gutierrez 2017) involved in carbonate precipitation inside the microbial mats to form dendrolites and leiolites. Briefly, the dendrolites with intergrowth of leiolites mostly dominated by filamentous cyanobacteria represented by *Epiphyton* (Figs. 5, 6, 7, 8, 9) and *Hedstroemia* (Fig. 10) in upper part of the Miaolingian Zhangxia Formation at the Aajiazhuang section might be generated by a sophisticated process, i.e. in-situ carbonate precipitation (Dupraz et al. 2009, 2011; Bosak et al. 2013) through decomposition of EPS mainly by sulfate-reducing bacteria to form a relatively thick microbial mat. The cyanobacteria are the most successful mat-building organisms that form microbial mats (biofilms) by secreting a mess of EPS (Stal 2012). Therefore, like stromatolites (Bosak et al. 2013), microbial reefs with thickness of more than 100 m (Fig. 3) in the study area, clarify the complex microbial process by the interactions of microbes with sediments, water energy and environments. However, as described by Dupraz et al. (2009, 2011) "*the greatest challenge that remains is the translation of all these processes and products in the fossil record and especially through the filter of the diagenesis*", numerous detailed problems related to forming mechanism of Miaolingian dendrolites and leiolites need further investigation in future.

Like the fenestral cavities filled by microspars within dense micrites of Miaolingian dendrolites ("F" in Fig. 5c, d) and leiolites (Fig. 15a), it depicts similar phenomena as observed in the Cambrian oncoids (Wilmeth et al. 2015), which might represent the residues of oxygen bubbles produced by photosynthesis in microbial mats (Bosak et al. 2010; Mata et al. 2012; Pepe-Ranney et al. 2012; Wilmeth et al. 2015; Mlewski et al. 2018). The fenestral cavities may also demonstrate that oxygen entrapped in the mat during the growth of dendrolites strengthens the hypothesis of the involvement of photosynthetic organisms in the formation of dendrolites (Wilmeth et al. 2015; Mlewski et al. 2018). Furthermore, special interstices within these large shrub-like thalli are chiefly composed of fossils of the *Epiphyton* group that depict characteristics of carbonate spars (Figs. 5a, b, 6, 7, 9) and might have similar origin as the photosynthetic oxygen bubbles in the spatial interstices of shrubs of the Miaolingian dendrolites during their growing period.

Although the fossils of *Epiphyton* group (Figs. 5, 6, 7, 8, 9, 13, 14, 15, 16) marked by bifurcating branches of dense micrites have been thought as red algal affinity (Luchinina and Terleev 2008, 2014; Luchinina 2009), their dense dark micritic composition clarifies that they have a similar origin to the *Girvanella* (Figs. 13e, 14 and 16) and the *Hedstroemia* (Fig. 10), i.e. in vivo calcification (Riding 1991b, 1991c, 2011b; Kah and Riding 2007) of structured sheaths that composed of special extracellular polymeric substances (EPSs; Dupraz et al. 2009, 2011; Decho 2010, 2011; Stal 2012; Tourney and Ngwenya 2014; Decho and Gutierrez 2017) with special protein of extracellular sunscreen scytonemins. Therefore, it is more reasonable to assign the fossils of the *Epiphyton* group into filamentous cyanobaceria. The distinctive bifurcating branches of the *Epiphyton* group forming shrubs in the Miaolingian dendrolites (Figs. 5, 6, 7, 8, 9) and leiolites (Figs. 12e, 13a, b, d, 14, 15, 16) may represent early examples of modularity (Suosaari et al. 2018), which further demonstrate that the microbial communities (mainly composed of filamentous cyanobacteria) are able to generate specific morphologies to increase the overall efficiency of network activity during the high-energy marine environment like the modern shrubs in living dendrolitic microbial mats in Hamelin Pool (Suosaari et al. 2018). Moreover, similar bifurcating branches formed by large *Lyngbya aestuarii* filaments in modern shrubs of living dendrolitic microbial mats that provide a modern analogue for the segmentated *Gordonophyton* of the *Epiphyton* group (Fig. 6a, c). Therefore, the example of shrubs in Miaolingain dendrolites also reflects biological habit of microbial communities that build them, and further provides insight into complex interplay of microbial communities and environment that not only broadens our understanding of dendrolite formation but also provides insight into detailed history of Early Paleozoic skeletal and microbial reefs (Rowland and Shapiro 2002; Kiessling 2009; McKenzie et al. 2014; Ezaki et al. 2017; Lee and Riding 2018; Cordie et al. 2019; Lee et al. 2019; Riding et al. 2019), and microbe–metazoan transitions of the Cambrian (Chen et al. 2019).

6 Conclusions

1) Microbial reefs with a thickness of more than 100 m are composed of dendrolites with the intergrowth of leiolites in upper part of the Miaolingian Zhangxia Formation at the Anjiazhuang section in Feicheng city of Shandong Province, grew on a high-energy oolitic-grain bank. It developed in a forced regressive systems tract of a third-order depositional sequence that is bounded by drowning uncorformities followed by sea-level rise.

These remarkable sedimentary deposits along with sophisticated microscopic features are reflected by diversified calcified cyanobacteria and the heterogeneous sedimentary fabrics.

2) The features of these rocks not only characterize the complexity of microbial reefs but also demonstrate the sophisticated mechanism of microbially-induced in-situ carbonate precipitation in multiple and relatively thick non-laminated microbial mat dominated by filamentous cyanobacteria. These deposits reflected several features such as: (i) shrub fabrics make up dendrolites chiefly dominated by filamentous cyanobacteria which are represented by *Epiphyton* and *Hedstroemia*; (ii) the special growing matrix for shrubs of dendrolites is marked by *Bacinella*-like fabric that can be grouped into a feature of modern microbialites (e.g. microbial mats), and the dense micrites may be considered as a result of $CaCO_3$ precipitation occurred simultaneously in metabolically active cyanobacterial layers; (iii) a possible colony of *Nostoc* is represented by the *Lithocodium*-like fabric within the dendrolites; (iv) *Epiphyton* and *Girvanella* intergrew within the leiolites; (v) the organic-mineralization of microbial mats is reflected by dolomitic cements within dendrolites and the chert lens inside the leiolites; and (vi) the sulfate reduction involved in carbonate precipitation within microbial mats forming these dendrolites and leiolites is reflected by pyritic residues.

3) Although many problems dealing with the forming mechanism and growth pattern for microbial reef complex dominated by dendrolites with intergrowth of leiolites in this study need further investigation, it provides a suitable example for further understanding of dendrolites with the intergrowth of leiolites built up by non-laminated cyanobacteria microbial mats. We hope that our observations and studies especially for the establishment of *Lithocodium* or the *Lithocodium*-like fabric during the Cambrian can provide some useful approaches and research clues for futher research and refine the history of Early Paleozoic skeletal reefs and the microbe–metazoan transitions of the Cambrian as well as further understanding of their driving factors in the future.

Abbrevations

DS: Depositional sequence; EPSs: Extracellular polymeric substances; MC: Microbial carbonate; MISSs: Microbially-induced sedimentary structures; PPL: Plain polarized light

Acknowledgements

We acknowledge Dr. Jing-Jing Li, for her support in understanding of microbial fossils in this research. We would like to thank doctors Xin-Wei Zhao, Sheng-Li Ni, Long Wang and Rui Zhang for their significant fieldwork contribution. Editor-in-chief Prof. Zeng-Zhao Feng is thanked for his critical comments and constructive suggestions to our original manuscript, which greatly improved the quality of the paper.

Authors' contributions

All the authors have actively participated in the preparation of this manuscript. MMX proposed the main concept and MR wrote the manuscript. These two researchers also collected field data. ZWZ, YH, and QFM assisted in establishing microfabrics, review and proofreading of the manuscript. The authors read and approved the final manuscript.

Funding

This study is funded by the National Natural Science Foundation of China (Grant No. 41472090).

Availability of data and materials

All relevant data and materials are presented in this published article.

Declarations

Competing interests

The authors declare that they have no competing interests.

Author details

[1]School of Earth Sciences and Resources, China University of Geosciences, Beijing 100083, China. [2]State Key Laboratory of Biogeology and Environmental Geology, China University of Geosciences, Beijing 100083, China. [3]State Key Laboratory of Oil and Gas Reservoir Geology and Exploitation, Chengdu University of Technology, Chengdu 610059, China. [4]College of Energy Resources, Chengdu University of Technology, Chengdu 610059, China. [5]Centre for Geographical Information System, University of the Punjab, Lahore 54590, Pakistan.

Received: 13 November 2019 Accepted: 4 March 2021
Published online: 20 March 2021

References

Adachi, N., A. Kotani, Y. Ezaki, and J.B. Liu. 2015. Cambrian Series 3 lithistid sponge–microbial reefs in Shandong Province, North China: Reef development after the disappearance of archaeocyaths. *Lethaia* 48 (3): 405–416. https://doi.org/10.1111/let.12118.

Adachi, N., T. Nakai, Y. Ezaki, and J.B. Liu. 2014. Late Early Cambrian archaeocyath reefs in Hubei Province, South China: Modes of construction during their period of demise. *Facies* 60 (2): 703–717. https://doi.org/10.1007/s10347-013-0376-y.

Aitken, J.D. 1967. Classification and environmental significance of cryptalgal limestones and dolomites, with illustrations from the Cambrian and Ordovician of southwestern Alberta. *Journal of Sedimentary Petrology* 37 (4): 1163–1178.

Bosak, T., J.W.M. Bush, M.R. Flynn, B. Liang, S. Ono, A.P. Petroff, and M.S. Sim. 2010. Formation and stability of oxygen-rich bubbles that shape photosynthetic mats. *Geobiology* 8 (1): 45–55. https://doi.org/10.1111/j.1472-4669.2009.00227.x.

Bosak, T., A.H. Knoll, and A.P. Petroff. 2013. The meaning of stromatolites. *Annual Review of Earth and Planetary Sciences* 41 (1): 21–44. https://doi.org/10.1146/annurev-earth-042711-105327.

Bosence, D., K. Gibbons, D.P. Le Heron, W.A. Morgan, T. Pritchard, and B.A. Vining. 2015. Microbial carbonates in space and time: Introduction. *Geological Society, London, Special Publications* 418 (1): 1–15. https://doi.org/10.1144/SP418.14.

Bostick, B.C. 2019. Massive ore deposits from microscopic organisms. *Geology* 47 (2): 191–192. https://doi.org/10.1130/focus022019.1.

Bradley, J.A., L.K. Daille, C.B. Trivedi, C.L. Bojanowski, B.W. Stamps, B.S. Stevenson, H.S. Nunn, H.A. Johnson, S.J. Loyd, W.M. Berelson, F.A. Corsetti, and J.R. Spear. 2017. Carbonate-rich dendrolitic cones: Insights into a modern analog for incipient microbialite formation, Little Hot Creek, Long Valley Caldera, California. *npj Biofilms and Microbiomes* 3 (1): 32 https://doi.org/10.1038/s41522-017-0041-2.

Braga, J.C., J.M. Martin, and R. Riding. 1995. Controls on microbial dome fabric development along a carbonate-siliciclastic shelf-basin transect, Miocene, SE Spain. *Palaios* 10 (4): 347–361. https://doi.org/10.2307/3515160.

Burne, R.V., and L.S. Moore. 1987. Microbialites: Organosedimentary deposits of benthic microbial communities. *Palaios* 2 (3): 241–254. https://doi.org/10.2307/3514674.

Burne, R.V., L.S. Moore, A.G. Christy, U. Troitzsch, P.L. King, A.M. Carnerup, and P.J. Hamilton. 2014. Stevensite in the modern thrombolites of Lake Clifton, Western Australia: A missing link in microbialite mineralization? *Geology* 42 (7): 575–578. https://doi.org/10.1130/G35484.1.

Chafetz, H.S., and S.A. Guidry. 1999. Bacterial shrubs, crystal shrubs, and ray-crystal shrubs: Bacterial vs. abiotic precipitation. *Sedimentary Geology* 126 (1-4): 57–74. https://doi.org/10.1016/S0037-0738(99)00032-9.

Chen, J.Y., Z.Z. Han, H.H. Fan, J.T. Chen, and N.J. Chi. 2014b. Characteristics and formation mechanism of Cambrian thrombolite in western Shandong Province. *Acta Geologica Sinica* 88 (6): 16–28 (in Chinese with English abstract).

Chen, J.Y., Z.Z. Han, H.H. Fan, and N.J. Chi. 2014a. Characteristics and sedimentary environment of thrombolite in the Zhangxia Formation (Third Series of Cambrian), Shandong Province. *Acta Sedimentologica Sinica* 32 (3): 494–502 (in Chinese with English abstract).

Chen, Z.Q., C.Y. Tu, Y. Pei, J. Ogg, Y.H. Fang, S.Q. Wu, X.Q. Feng, Y.G. Huang, Z. Guo, and H. Yang. 2019. Biosedimentological features of major microbe-metazoan transitions (MMTs) from Precambrian to Cenozoic. *Earth-Science Reviews* 189: 21–50. https://doi.org/10.1016/j.earscirev.2019.01.015.

Cherchi, A., and R. Schroeder. 2006. Remarks on the systematic position of *Lithocodium* Elliott, a problematic microorganism from the Mesozoic carbonate platforms of the Tethyan realm. *Facies* 52 (3): 435–440. https://doi.org/10.1007/s10347-006-0045-5.

Choquette, P.W., and E.E. Hiatt. 2008. Shallow-burial dolomite cement: A major component of many ancient sucrosic dolomites. *Sedimentology* 55 (2): 423–460. https://doi.org/10.1111/j.1365-3091.2007.00908.x.

Cordie, D.R., S.Q. Dornbos, P.J. Marenco, T. Oji, and S. Gonchigdorj. 2019. Depauperate skeletonized reef-dwelling fauna of the Early Cambrian: Insights from archaeocyathan reef ecosystems of western Mongolia. *Palaeogeography, Palaeoclimatology, Palaeoecology* 514: 206–221. https://doi.org/10.1016/j.palaeo.2018.10.027.

Coulson, K.P., and L.R. Brand. 2016. Lithistid sponge-microbial reef-building communities construct laminated, upper Cambrian (Furongian) 'stromatolites'. *Palaios* 31 (7): 358–370. https://doi.org/10.2110/palo.2016.029.

De los Ríos, A., C. Ascaso, J. Wierzchos, W.F. Vincent, and A. Quesada. 2015. Microstructure and cyanobacterial composition of microbial mats from the high Arctic. *Biodiversity and Conservation* 24 (4): 841–863. https://doi.org/10.1007/s10531-015-0907-7.

Decho, A.W. 2010. Overview of biopolymer-induced mineralization: What goes on in biofilms? *Ecological Engineering* 36 (2): 137–144. https://doi.org/10.1016/j.ecoleng.2009.01.003.

Decho, A.W. 2011. Extracellular polymeric substances (EPS). In *Encyclopedia of Geobiology*, ed. J. Reitner and V. Thiel, 359–362. Berlin, Heidelberg: Springer-Verlag. https://doi.org/10.1007/978-1-4020-9212-1_86.

Decho, A.W., and T. Gutierrez. 2017. Microbial extracellular polymeric substances (EPSs) in ocean systems. *Frontiers in Microbiology* 8: 922 https://doi.org/10.3389/fmicb.2017.00922.

Dupraz, C., R.P. Reid, O. Braissant, A.W. Decho, R.S. Norman, and P.T. Visscher. 2009. Processes of carbonate precipitation in modern microbial mats. *Earth-Science Reviews* 96 (3): 141–162. https://doi.org/10.1016/j.earscirev.2008.10.005.

Dupraz, C., R.P. Reid, and P.T. Visscher. 2011. Microbialites, modern. In *Encyclopedia of Geobiology*, ed. J. Reitner and V. Thiel, 617–635. Berlin, Heidelberg: Springer-Verlag. https://doi.org/10.1007/978-1-4020-9212-1_195.

Elliott, G.F. 1956. Further records of fossil calcareous algae from the Middle East. *Micropaleontology* 2 (4): 327–334. https://doi.org/10.2307/1484348.

Ezaki, Y., J.B. Liu, N. Adachi, and Z. Yan. 2017. Microbialite development during the protracted inhibition of skeletal-dominated reefs in the Zhangxia Formation (Cambrian Series 3) in Shandong Province, North China. *Palaios* 32 (9): 559–571. https://doi.org/10.2110/palo.2016.097.

Feng, Z.Z., Y.M. Peng, Z.K. Jin, P.L. Jiang, and Z.D. Bao. 2004. *Lithofacies Palaeogeography of the Cambrian and Ordovician in China*, 112–121. Beijing: Petroleum Industry Press (in Chinese).

Feng, Z.Z., Y.H. Wang, J.S. Zhang, W.Q. Zuo, X.L. Zhang, G.L. Hong, J.X. Chen, S.H. Wu, Y.T. Chen, Y.L. Chi, and C.Y. Yang. 1990. *Lithofacies Palaeogeography of the Early Paleozoic of North China Platform*, pp. 28–48. Beijing: Geological Publishing House (in Chinese).

Flemming, H.C., and J. Wingender. 2010. The biofilm matrix. *Nature Reviews Microbiology* 8 (9): 623–633. https://doi.org/10.1038/nrmicro2415.

Flemming, H.C., J. Wingender, U. Szewzyk, P. Steinberg, S.A. Rice, and S. Kjelleberg. 2016. Biofilms: An emergent form of bacterial life. *Nature Reviews Microbiology* 14 (9): 563–575. https://doi.org/10.1038/nrmicro.2016.94.

Gallagher, K.L., T.J. Kading, O. Braissant, C. Dupraz, and P.T. Visscher. 2012. Inside the alkalinity engine: The role of electron donors in the organomineralization potential of sulfate-reducing bacteria. *Geobiology* 10 (6): 518–530. https://doi.org/10.1111/j.1472-4669.2012.00342.x.

Gerdes, G. 2010. What are microbial mats? In *Microbial Mats: Modern and Ancient Microorganisms in Stratified Systems*, ed. J. Seckbach and A. Oren, 5–25. Berlin, Heidelberg: Springer-Verlag.

Gómez, J.J., and S. Fernández-López. 1994. Condensation processes in shallow platforms. *Sedimentary Geology* 92 (3–4): 147–159. https://doi.org/10.1016/0037-0738(94)90103-1.

Gong, Y.Y. 2016. Sedimentary fabrics for the Cambrian thrombolite bioherm: An example from the Zhangxia Formation in western Shandong Province. *Geoscience* 30 (2): 436–444 (in Chinese with English abstract).

Gregg, J.M., D.L. Bish, S.E. Kaczmarek, and H.G. Machel. 2015. Mineralogy, nucleation and growth of dolomite in the laboratory and sedimentary environment: A review. *Sedimentology* 62 (6): 1749–1769. https://doi.org/10.1111/sed.12202.

Han, Z.Z., J.T. Chen, X.L. Zhang, and X.F. Yu. 2009. Characteristics of *Epiphyton* and *Epiphyton* microbialites in the Zhangxia Formation (Third Series of Cambrian), Shandong Province. *Acta Geologica Sinica* 83 (8): 1097–1103 (in Chinese with English abstract).

Helm, R.F., and M. Potts. 2012. Extracellular matrix (ECM). In *Ecology of Cyanobacteria II: Their Diversity in Space and Time*, ed. B.A. Whitton, 461–480. Netherlands: Springer.

Howell, J., J. Woo, and S.K. Chough. 2011. Dendroid morphology and growth patterns: 3-D computed tomographic reconstruction. *Palaeogeography, Palaeoclimatology, Palaeoecology* 299 (1–2): 335–347. https://doi.org/10.1016/j.palaeo.2010.11.013.

Hunt, D., and M.E. Tucker. 1992. Stranded parasequences and the forced regressive wedge systems tract: Deposition during base-level fall. *Sedimentary Geology* 81 (1): 1–9. https://doi.org/10.1016/0037-0738(92)90052-S.

Jiang, M.S., and Q.A. Sha. 1996. Algal limestones and their sedimentary fabrics in the Zhangxia Formation (Middle Cambrian), North Jiangsu–West Shandong region. *Sedimentary Facies and Palaeogeography* 16 (5): 12–17 (in Chinese with English abstract).

Kah, L.C., and R. Riding. 2007. Mesoproterozoic carbon dioxide levels inferred from calcified cyanobacteria. *Geology* 35 (9): 799–802. https://doi.org/10.1130/G23680A.1.

Kaźmierczak, J., T. Fenchel, M. Kühl, S. Kempe, B. Kremer, B. Łącka, and K. Małkowski. 2015. $CaCO_3$ precipitation in multilayered cyanobacterial mats: Clues to explain the alternation of micrite and sparite layers in calcareous stromatolites. *Life* 5 (1): 744–769. https://doi.org/10.3390/life5010744.

Kennard, J.M., and N.P. James. 1986. Thrombolites and stromatolites: Two distinct types of microbial structures. *Palaios* 1 (5): 492–503. https://doi.org/10.2307/3514631.

Kiessling, W. 2009. Geologic and biologic controls on the evolution of reefs. *Annual Review of Ecology, Evolution, and Systematics* 40 (1): 173–192. https://doi.org/10.1146/annurev.ecolsys.110308.120251.

Kruse, P.D., and J.R. Reitner. 2014. Northern Australian microbial-metazoan reefs after the mid-Cambrian mass extinction. *Memoirs of the Association of Australasian Palaeontologists* 45 (45): 31–53.

Kwon, S.W., J. Park, S.J. Choh, D.C. Lee, and D.J. Lee. 2012. Tetradiid-siliceous sponge patch reefs from the Xiazhen Formation (late Katian), Southeast China: A new Late Ordovician reef association. *Sedimentary Geology* 267–268: 15–24.

Larmagnat, S., and F. Neuweiler. 2015. Taphonomic filtering in Ordovician bryozoan carbonate mounds, Trenton group, Montmorency falls, Quebec, Canada. *Palaios* 30 (3): 169–180. https://doi.org/10.2110/palo.2013.120.

Latif, K., E.Z. Xiao, M. Riaz, L. Wang, M.Y. Khan, A.A. Hussein, and M.U. Khan. 2018. Sequence stratigraphy, sea-level changes and depositional systems in the Cambrian of the North China Platform: A case study of Kouquan section, Shanxi Province, China. *Journal of Himalayan Earth Sciences* 51 (1): 1–16.

Laval, B., S.L. Cady, J.C. Pollack, C.P. McKay, J.S. Bird, J.P. Grotzinger, D.C. Ford, and H.R. Bohm. 2000. Modern freshwater microbialite analogues for ancient dendritic reef structures. *Nature* 407 (6804): 626–629. https://doi.org/10.1038/35036579.

Lee, J.H., J.T. Chen, S.J. Choh, D.J. Lee, Z.Z. Han, and S.K. Chough. 2014a. Furongian (Late Cambrian) sponge–microbial maze-like reefs in the North China Platform. *Palaios* 29 (1): 27–37. https://doi.org/10.2110/palo.2013.050.

Lee, J.H., J.T. Chen, and S.K. Chough. 2015. The Middle–Late Cambrian reef transition and related geological events: A review and new view. *Earth-Science Reviews* 145: 66–84. https://doi.org/10.1016/j.earscirev.2015.03.002.

Lee, J.H., B.F. Dattilo, S. Mrozek, J.F. Miller, and R. Riding. 2019. Lithistid sponge-microbial reefs, Nevada, USA: Filling the Late Cambrian 'reef gap'. *Palaeogeography, Palaeoclimatology, Palaeoecology* 520: 251–262. https://doi.org/10.1016/j.palaeo.2019.02.003.

Lee, J.H., H.S. Lee, J. Chen, J. Woo, and S.K. Chough. 2014b. Calcified microbial reefs in Cambrian Series 2, North China Platform: Implications for the evolution of Cambrian calcified microbes. *Palaeogeography, Palaeoclimatology, Palaeoecology* 403: 30–42. https://doi.org/10.1016/j.palaeo.2014.03.020.

Lee, J.H., and R. Riding. 2018. Marine oxygenation, lithistid sponges, and the early history of Paleozoic skeletal reefs. *Earth-Science Reviews* 181: 98–121. https://doi.org/10.1016/j.earscirev.2018.04.003.

Lee, J.H., J. Woo, and D.J. Lee. 2016. The earliest reef-building anthaspidellid sponge *Rankenella zhangxianensis* n. sp. from the Zhangxia Formation (Cambrian Series 3), Shandong Province, China. *Journal of Paleontology* 90 (1): 1–9. https://doi.org/10.1017/jpa.2015.53.

Li, Q.J., Y. Li, J.P. Wang, and W. Kiessling. 2015. Early Ordovician lithistid sponge–*Calathium* reefs on the Yangtze Platform and their paleoceanographic implications. *Palaeogeography, Palaeoclimatology, Palaeoecology* 425: 84–96. https://doi.org/10.1016/j.palaeo.2015.02.034.

Lin, C.Y., A.V. Turchyn, Z. Steiner, P. Bots, G.I. Lampronti, and N.J. Tosca. 2018. The role of microbial sulfate reduction in calcium carbonate polymorph selection. *Geochimica et Cosmochimica Acta* 237: 184–204. https://doi.org/10.1016/j.gca.2018.06.019.

Liu, L.J., Y.S. Wu, H.X. Jiang, and R. Riding. 2016. Calcified rivulariaceans from the Ordovician of the Tarim Basin, Northwest China, Phanerozoic lagoonal examples, and possible controlling factors. *Palaeogeography, Palaeoclimatology, Palaeoecology* 448: 371–381. https://doi.org/10.1016/j.palaeo.2015.08.034.

Lu, Y.H., W.T. Zhang, Z.L. Zhu, L.W. Xiang, H.L. Lin, Z.Y. Zhou, J.L. Yuan, S.C. Peng, Y. Qian, S.G. Zhang, S.J. Li, H.J. Guo, and H.L. Luo. 1994. Suggestions for the establishment of the Cambrian stages in China. *Journal of Stratigraphy* 18 (4): 318–328 (in Chinese with English abstract).

Luchinina, V.A. 2009. *Remalcis* and *Epiphyton* as different stages in the life cycle of calcareous algae. *Paleontological Journal* 43 (4): 463–468. https://doi.org/10.1134/S0031030109040169.

Luchinina, V.A., and A.A. Terleev. 2008. The morphology of the genus *Epiphyton* Bornemann. *Geologia Croatica* 61 (2–3): 105–111.

Luchinina, V.A., and A.A. Terleev. 2014. Features of calcareous algae mineralization at the transition to the Phanerozoic biosphere. *Paleontological Journal* 48 (14): 1450–1456. https://doi.org/10.1134/S0031030114007X.

Luo, C., and J. Reitner. 2014. First report of fossil "keratose" demosponges in Phanerozoic carbonates: Preservation and 3-D reconstruction. *Naturwissenschaften* 101 (6): 467–477. https://doi.org/10.1007/s00114-014-1176-0.

Luo, C., and J. Reitner. 2016. 'Stromatolites' built by sponges and microbes — A new type of Phanerozoic bioconstruction. *Lethaia* 49 (4): 555–570. https://doi.org/10.1111/let.12166.

Ma, Y.S., M.X. Mei, R.X. Zhou, and W. Yang. 2017. Forming patterns for the oolitic bank within the sequence-stratigraphic framework: An example from the Cambrian series 3 at the Xiaweidian section in the western suburb of Beijing. *Acta Petrologica Sinica* 33 (4): 1021–1036 (in Chinese with English abstract).

Mata, S.A., C.L. Harwood, F.A. Corsetti, N.J. Stork, K. Eilers, W.M. Berelson, and J.R. Spear. 2012. Influence of gas production and filament orientation on stromatolite microfabric. *Palaios* 27 (4): 206–219. https://doi.org/10.2110/palo.2011.p11-088r.

Mazzullo, S.J. 2000. Organogenic dolomitization in peritidal to deep-sea sediments. *Journal of Sedimentary Research* 70 (1): 10–23. https://doi.org/10.1306/2DC408F9-0E47-11D7-8643000102C1865D.

McKenzie, N.R., N.C. Hughes, B.C. Gill, and P.M. Myrow. 2014. Plate tectonic influences on Neoproterozoic–Early Paleozoic climate and animal evolution. *Geology* 42 (2): 127–130. https://doi.org/10.1130/G34962.1.

Mei, M.X. 1996. Carbonate third-order cyclic sequence of the drowning-unconformity type: Discussion on the condensation of carbonate platform. *Sedimentary Facies and Palaeogeography* 16 (6): 24–33 (in Chinese with English abstract).

Mei, M.X. 2010. Correlation of sequence boundaries according to discerning between normal and forced regressions: The first advance in sequence stratigraphy. *Journal of Palaeography (Chinese Edition)* 12 (5): 549–564 (in Chinese with English abstract).

Mei, M.X. 2011a. Depositional trends and sequence-stratigraphic successions under the Cambrian second-order transgressive setting in the North China platform: A case study of the Xiaweidian section in the western suburb of Beijing. *Geology in China* 38 (2): 317–337 (in Chinese with English abstract).

Mei, M.X. 2011b. Microbial-mat sedimentology: A young branch from sedimentology. *Advances in Earth Science* 26 (6): 586–597 (in Chinese with English abstract).

Mei, M.X. 2012. Brief introduction of "dolostone problem" in sedimentology according to three scientific ideas. *Journal of Palaeogeography (Chinese Edition)* 14 (1): 1–12 (in Chinese with English abstract).

Mei, M.X. 2014. Feature and nature of microbial-mat: Theoretical basis of microbial-mat sedimentology. *Journal of Palaeography (Chinese Edition)* 16 (3): 285–304 (in Chinese with English abstract).

Mei, M.X., K. Latif, C.J. Mei, J.H. Gao, and Q.F. Meng. 2020. Thrombolitic clots dominated by filamentous cyanobacteria and crusts of radio-fibrous calcite in the Furongian Changshan Formation, North China. *Sedimentary Geology* 395: 105540 https://doi.org/10.1016/j.sedgeo.2019.105540.

Mei, M.X., and X.D. Yang. 2000. Forced regression and forced regressive wedge system tract: Revision on traditional Exxon model of sequence stratigraphy. *Geological Science and Technology Information* 19 (2): 17–21 (in Chinese with English abstract).

Mei, M.X., R. Zhang, Y.Y. Li, and L. Jie. 2017. Calcified cyanobacterias within the stromatolotic bioherm for the Cambrian Furongian Series in the northeastern margin of the North-China Platform. *Acta Petrologica Sinica* 33 (4): 1073–1093 (in Chinese with English abstract).

Meng, X.H., M. Ge, and M.E. Tucker. 1997. Sequence stratigraphy, sea-level changes and depositional systems in the Cambro-Ordovician of the North China carbonate platform. *Sedimentary Geology* 114 (1-4): 189–222. https://doi.org/10.1016/S0037-0738(97)00073-0.

Miller, C.R., and N.P. James. 2012. Autogenic microbial genesis of middle Miocene palustrine ooids, Nullarbor Plain, Australia. *Journal of Sedimentary Research* 82 (9): 633–647. https://doi.org/10.2110/jsr.2012.60.

Mlewski, E.C., C. Pisapia, F. Gomez, L. Lecourt, E. Soto Rueda, K. Benzerara, B. Ménez, S. Borensztajn, F. Jamme, M. Réfrégiers, and E. Gérard. 2018. Characterization of pustular mats and related *Rivularia*-rich laminations in oncoids from the Laguna Negra Lake (Argentina). *Frontiers in Microbiology* 9: 996 https://doi.org/10.3389/fmicb.2018.00996.

Mohr, K.I., N. Brinkmann, and T. Friedl. 2011. Cyanobacteria. In *Encyclopedia of Geobiology*, ed. J. Reitner and V. Thiel, 306–311. Berlin, Heidelberg: Springer-Verlag.

Noffke, N., and S.M. Awramik. 2013. Stromatolites and MISS: Differences between relatives. *GSA Today* 23 (9): 4–9. https://doi.org/10.1130/GSATG187A.1.

Pacton, M., D. Ariztegui, D. Wacey, M.R. Kilburn, C. Rollion-Bard, R. Farah, and C. Vasconcelos. 2012. Going nano: A new step toward understanding the processes governing freshwater ooid formation. *Geology* 40 (6): 547–550. https://doi.org/10.1130/G32846.1.

Park, J., J.H. Lee, J. Hong, S.J. Choh, D.C. Lee, and D.J. Lee. 2015. An Upper Ordovician sponge-bearing micritic limestone and implication for Early Palaeozoic carbonate successions. *Sedimentary Geology* 319: 124–133. https://doi.org/10.1016/j.sedgeo.2015.02.002.

Peng, S.C. 2009. Review on the studies of Cambrian trilobite faunas from Jiangnan slope belt, South China, with notes on Cambrian correlation between south and North China. *Acta Palaeontologica Sinica* 48: 437–452 (in Chinese with English abstract).

Peng, S.C., and Y.L. Zhao. 2018. The proposed global standard stratotype-section and point (GSSP) for the conterminous base of Miaolingian series and Wuliuan stage at Balang, Jianhe, Guizhou, China was ratified by IUGS. *Journal of Stratigraphy* 42 (3): 325–327 (in Chinese with English abstract).

Pepe-Ranney, C., W.M. Berelson, F.A. Corsetti, M. Treants, and J.R. Spear. 2012. Cyanobacterial construction of hot spring siliceous stromatolites in Yellowstone national Park. *Environmental Microbiology* 14 (5): 1182–1197. https://doi.org/10.1111/j.1462-2920.2012.02698.x.

Perri, E., M.E. Tucker, M. Słowakiewicz, F. Whitaker, L. Bowen, and I.D. Perrotta. 2018. Carbonate and silicate biomineralization in a hypersaline microbial mat (Mesaieed sabkha, Qatar): Roles of bacteria, extracellular polymeric substances and viruses. *Sedimentology* 65 (4): 1213–1245. https://doi.org/10.1111/sed.12419.

Peters, S.E., and R.R. Gaines. 2012. Formation of the 'great unconformity' as a trigger for the Cambrian explosion. *Nature* 484 (7394): 363–366. https://doi.org/10.1038/nature10969.

Potts, M. 1997. Etymology of the genus name *Nostoc* (cyanobacteria). *International Journal of Systematic and Evolutionary Microbiology* 47 (2): 584 https://doi.org/10.1099/00207713-47-2-584.

Pratt, B.R., M.M. Raviolo, and O.L. Bordonaro. 2012. Carbonate platform dominated by peloidal sands: Lower Ordovician La Silla Formation of the eastern Precordillera, San Juan, Argentina. *Sedimentology* 59 (3): 843–866. https://doi.org/10.1111/j.1365-3091.2011.01282.x.

Qi, Y.A., Y.P. Wang, M.Y. Dai, and D. Li. 2014. Thrombolites and controlling factors from the Zhangxia Formation of Cambrian Series 3 in Dengfeng, western Henan Province. *Acta Micropalaeontologica Sinica* 31 (3): 243–255 (in Chinese with English abstract).

Radoičić, R. 1959. Nekoliko problematičnih mikrofosila iz dinarske krede (some problematic microfossils from the Dinarian cretaceous). *Bulletin du Service Géologique et Géophysique RP Serbie* 17: 87–92.

Rameil, N., A. Immenhauser, G. Warrlich, H. Hillgärtner, and H.J. Droste. 2010. Morphological patterns of Aptian *Lithocodium–Bacinella* geobodies: Relation to environment and scale. *Sedimentology* 57 (3): 883–911. https://doi.org/10.1111/j.1365-3091.2009.01124.x.

Reitner, J. 2011a. Biofilm. In *Encyclopedia of Geobiology*, ed. J. Reitner and V. Thiel, 134–135. Berlin, Heidelberg: Springer-Verlag.

Reitner, J. 2011b. Microbial mats. In *Encyclopedia of Geobiology*, ed. J. Reitner and V. Thiel, 606–608. Berlin, Heidelberg: Springer-Verlag.

Riaz, M., K. Latif, T. Zafar, E.Z. Xiao, S. Ghazi, L. Wang, and A.A. Hussein. 2019b. Assessment of Cambrian sequence stratigraphic style of the North China Platform exposed in Wuhai division, Inner Mongolia. *Himalayan Geology* 40 (1): 92–102.

Riaz, M., E.Z. Xiao, K. Latif, and T. Zafar. 2019a. Sequence-stratigraphic position of oolitic bank of Cambrian in North China platform: Example from the Kelan section of Shanxi Province. *Arabian Journal for Science and Engineering* 44 (1): 391–407. https://doi.org/10.1007/s13369-018-3403-z.

Riaz, M., T. Zafar, K. Latif, S. Ghazi, and E.Z. Xiao. 2020. Petrographic and rare earth elemental characteristics of Cambrian *Girvanella* oncoids exposed in the North China Platform: Constraints on forming mechanism, REE sources, and paleoenvironments. *Arabian Journal of Geosciences* 13 (17): 858 https://doi.org/10.1007/s12517-020-05750-8.

Rickard, D., M. Mussmann, and J.A. Steadman. 2017. Sedimentary sulfides. *Elements* 13 (2): 117–122. https://doi.org/10.2113/gselements.13.2.117.

Riding, R. 1991a. Classification of microbial carbonates. In *Calcareous Algae and Stromatolites*, ed. R. Riding, 21–51. Berlin: Springer-Verlag.

Riding, R. 1991b. Calcified cyanobacteria. In *Calcareous Algae and Stromatolites*, ed. R. Riding, 55–87. Berlin: Springer-Verlag.

Riding, R. 1991c. Cambrian calcareous cyanobacteria and algae. In *Calcareous Algae and Stromatolites*, ed. R. Riding, 305–334. Berlin: Springer-Verlag.

Riding, R. 2000. Microbial carbonates: The geological record of calcified bacterial–algal mats and biofilms. *Sedimentology* 47 (s1): 179–214. https://doi.org/10.1046/j.1365-3091.2000.00003.x.

Riding, R. 2002a. Structure and composition of organic reefs and carbonate mud mounds: Concepts and categories. *Earth-Science Reviews* 58 (1–2): 163–231. https://doi.org/10.1016/S0012-8252(01)00089-7.

Riding, R. 2002b. Biofilm architecture of Phanerozoic cryptic carbonate marine veneers. *Geology* 30 (1): 31–34. https://doi.org/10.1130/0091-7613(2002)030<0031:BAOPCC>2.0.CO;2.

Riding, R. 2011a. Microbialites, stromatolites, and thrombolites. In *Encyclopedia of Geobiology*, ed. J. Reitner and V. Thiel, 635–654. Berlin, Heidelberg: Springer-Verlag.

Riding, R. 2011b. Calcified cyanobacteria. In *Encyclopedia of Geobiology*, ed. J. Reitner and V. Thiel, 211–223. Berlin, Heidelberg: Springer-Verlag.

Riding, R., L.Y. Liang, J.H. Lee, and A. Virgone. 2019. Influence of dissolved oxygen on secular patterns of marine microbial carbonate abundance during the past 490 Myr. *Palaeogeography, Palaeoclimatology, Palaeoecology* 514: 135–143. https://doi.org/10.1016/j.palaeo.2018.10.006.

Roberts, J.A., P.A. Kenward, D.A. Fowle, R.H. Goldstein, L.A. González, and D.S. Moore. 2013. Surface chemistry allows for abiotic precipitation of dolomite at low temperature. *Proceedings of the National Academy of Sciences* 110 (36): 14540–14545. https://doi.org/10.1073/pnas.1305403110.

Rowland, S.M., and R.S. Shapiro. 2002. Reef patterns and environmental influences in the Cambrian and earliest Ordovician. In *Phanerozoic Reef Patterns*, ed. W. Kiessling, E. Flügel, and J. Golonka, 95–128. Tulsa: Society of Economic Paleontologists and Mineralogists, special publications 72.

Săsăran, E., I.I. Bucur, G. Pleş, and R. Riding. 2014. Late Jurassic *Epiphyton*-like cyanobacteria: Indicators of long-term episodic variation in marine bioinduced microbial calcification? *Palaeogeography, Palaeoclimatology, Palaeoecology* 401: 122–131. https://doi.org/10.1016/j.palaeo.2014.02.026.

Schlager, W. 1989. Drowning unconformities on carbonate platforms. In *Controls on Carbonate Platform and Basin Development*, ed. P.D. Crevello, J.L. Wilson, J.F. Sarg, and J.F. Read, 15–25. Tulsa: Society of Economic Paleontologists and Mineralogists, special publications 44.

Schlager, W. 1998. Exposure, drowning and sequence boundaries on carbonate platforms. In *Reefs and Carbonate Platforms in the Pacific and Indian Oceans*, ed. G. Camoin and P. Davies, 3–21. International Association of Sedimentologists, special publications 25.

Schlager, W. 1999. Type 3 sequence boundaries. In *Carbonate Sequence Stratigraphy: Application to Reservoirs, Outcrops and Models*, ed. P. Harris, A. Saller, and A. Simo, 35–46. Tulsa: Society of Economic Paleontologists and Mineralogists, special publications 63.

Schlager, W., and G. Warrlich. 2009. Record of sea-level fall in tropical carbonates. *Basin Research* 21 (2): 209–224. https://doi.org/10.1111/j.1365-2117.2008.00383.x.

Schlagintweit, F., and T. Bover-Arnal. 2013. Remarks on *Bačinella* Radoičić, 1959 (type species *B. irregularis*) and its representatives. *Facies* 59 (1): 59–73. https://doi.org/10.1007/s10347-012-0309-1.

Schlagintweit, F., T. Bover-Arnal, and R. Salas. 2010. New insights into *Lithocodium aggregatum* Elliott 1956 and *Bacinella irregularis* Radoičić 1959 (Late Jurassic–Lower Cretaceous): Two ulvophycean green algae (?Order Ulotrichales) with a heteromorphic life cycle (epilithic/euendolithic). *Facies* 56 (4): 509–547. https://doi.org/10.1007/s10347-010-0222-4.

Schmid, D.U., and R.R. Leinfelder. 1996. The Jurassic *Lithocodium aggregatum–Troglotella incrustans* foraminiferal consortium. *Palaeontology* 39 (1): 21–52.

Sha, Q.A., and M.S. Jiang. 1998. The deposits of oolitic shoal facies and algal flat facies: Dissect of the Zhangxia Formation of the Middle Cambrian, western Shandong Province. *Acta Sedimentologica Sinica* 16 (4): 62–70 (in Chinese with English abstract).

Shen, Y.F., and F. Neuweiler. 2018. Questioning the microbial origin of automicrite in Ordovician calathid–demosponge carbonate mounds. *Sedimentology* 65 (1): 303–333. https://doi.org/10.1111/sed.12394.

Shi, X.Y., J.Q. Chen, and S.L. Mei. 1997. Cambrian sequence chronostratigraphic framework of the North China Platform. *Earth Science Frontiers* 4 (3–4): 165–177 (in Chinese with English abstract).

Soule, T., F. Garcia-Pichel, and V. Stout. 2009. Gene expression patterns associated with the biosynthesis of the sunscreen scytonemin in *Nostoc punctiforme* ATCC 29133 in response to UVA radiation. *Journal of Bacteriology* 191 (14): 4639–4646. https://doi.org/10.1128/JB.00134-09.

Stal, L.J. 2012. Cyanobacterial mats and stromatolites. In *Ecology of Cyanobacteria II: Their Diversity in Space and Time*, ed. B.A. Whitton, 65–125. Netherlands: Springer.

Suosaari, E.P., S.M. Awramik, R.P. Reid, J.F. Stolz, and K. Grey. 2018. Living dendrolitic microbial mats in Hamelin Pool, Shark Bay, Western Australia. *Geosciences* 8 (6): 212–229. https://doi.org/10.3390/geosciences8060212.

Tourney, J., and B.T. Ngwenya. 2014. The role of bacterial extracellular polymeric substances in geomicrobiology. *Chemical Geology* 386: 115–132. https://doi.org/10.1016/j.chemgeo.2014.08.011.

Védrine, S., A. Strasser, and W. Hug. 2007. Oncoid growth and distribution controlled by sea-level fluctuations and climate (late Oxfordian, Swiss Jura Mountains). *Facies* 53 (4): 535–552. https://doi.org/10.1007/s10347-007-0114-4.

Wang, Y.H., X.L. Zhang, and C.Y. Yang. 1989. *Carbonate Rocks for the Early Paleozoic of the North China Platform*, 133 pp. Beijing: Seismological Press (in Chinese).

Whitton, B.A., and P. Mateo. 2012. Rivulariaceae. In *Ecology of Cyanobacteria II: Their Diversity in Space and Time*, ed. B.A. Whitton, 561–591. Netherlands: Springer.

Wilmeth, D.T., F.A. Corsetti, N. Bisenic, S.Q. Dornbos, T. Oji, and S. Gonchigdorj. 2015. Punctuated growth of microbial cones within Early Cambrian oncoids, Bayan Gol Formation, western Mongolia. *Palaios* 30 (12): 836–845. https://doi.org/10.2110/palo.2015.014.

Woo, J., and S.K. Chough. 2010. Growth patterns of the Cambrian microbialite: Phototropism and speciation of *Epiphyton*. *Sedimentary Geology* 229 (1–2): 1–8. https://doi.org/10.1016/j.sedgeo.2010.05.006.

Woo, J., S.K. Chough, and Z. Han. 2008. Chambers of *Epiphyton* thalli in microbial buildups, Zhangxia Formation (Middle Cambrian), Shandong Province, China. *Palaios* 23 (1): 55–64. https://doi.org/10.2110/palo.2006.p06-103r.

Wright, D.J., S.C. Smith, V. Joardar, S. Scherer, J. Jervis, A. Warren, R.F. Helm, and M. Potts. 2005. UV irradiation and desiccation modulate the three-dimensional extracellular matrix of *Nostoc commune* (cyanobacteria). *Journal of Biological Chemistry* 280 (48): 40271–40281. https://doi.org/10.1074/jbc.M505961200.

Xiang, L.W., Z.I. Zhu, S.J. Li, and Z.Q. Zhou. 1999. *Stratigraphical lexicon of China: Cambrian*. Beijing: Geological Publishing House (in Chinese).

Yan, Z., J.B. Liu, Y. Ezaki, N. Adachi, and S.X. Du. 2017. Stacking patterns and growth models of multiscopic structures within Cambrian series 3 thrombolites at the Jiulongshan section, Shandong Province, northern China. *Palaeogeography, Palaeoclimatology, Palaeoecology* 474: 45–57. https://doi.org/10.1016/j.palaeo.2016.07.009.

Zhang, J.M., Y.K. Zhou, and Z.Z. Wang. 1985. *Epiphyton* boundstone and palaeogeography of the Middle Cambrian Zhangxia Formation in the east of North China Platform. *Acta Sedimentologica Sinica* 3 (1): 63–70 (in Chinese with English abstract).

Publisher's Note